Robert STRIEMITZER, BSc

Contamination-free immersion approaches for Raman microscopy

Master's Thesis

to achieve the university degree of

Diplom-Ingenieur

Master's degree programme: Technical Physics

submitted to

Graz University of Technology

Supervisor:

Ao.Univ.-Prof. Dipl.-Ing. Dr.techn. Ferdinand Hofer

Institute of Electron Microscopy and Nanoanalysis

Graz, 13.03. 2020

Affidavit

I declare that I have authored this thesis independently, that I have not used other than the declared sources/resources, and that I have explicitly indicated all material which has been quoted either literally or by content from the sources used. The text document uploaded to TUGRAZonline is identical to the present doctoral thesis.

_____	_____
Date	Signature

Acknowledgement

Diese Arbeit repräsentiert das Ende einer Studienzeit die schöner, aber auch nicht länger hätte sein können. Durch zahlreiche Gründe war sie oft unterbrochen und wurde verlängert, aber endet nun endlich mit dieser Arbeit was ohne die Mithilfe und Unterstützung akademischer oder anderer Natur nicht möglich gewesen wäre. Die Liste der Unterstützer, Professoren, Mitstudierenden, Freunden und Familienmitgliedern ist lang und ich bin mir sicher, dass ich jemanden vergesse wofür ich um Verzeihung bitte.

Ich bedanke mich bei Prof. Hofer für die Übernahme der Betreuung dieser Arbeit und bei Prof. Pölt für die ursprüngliche Betreuung. Harald Fitzek hat mich über die gesamte Dauer meiner Arbeit stehts unterstützt wofür ich äußerst dankbar bin. Ebenso bedanke ich mich beim gesamten Team, Diplomanten und Dissertanten des FELMI/ZFE für die Unterstützung bei Organisatorischem und die angenehme Zeit am Institut.

Ich bedanke mich bei meiner Mutter für jegliche Unterstützung zeitlebens. Ohne dich hätte ich mein Studium schön früher beendet, bzw. beenden müssen. Weiters bedanke ich mich bei meinem Vater, ohne den ich heute nicht der Mensch wäre, der ich heute bin.

Abschließend bedanke ich mich bei all meinen Freunden. Allen Freunden, die ich seit Kindheitstagen habe und immer an meiner Seite waren; allen, die mich auf Stücken des Weges begleitet haben und allen, die ich dazu gewinnen durfte und mir hoffentlich noch lange erhalten bleiben: Flo, Willi, Peter, Gideon, Martin, Nina, Julian, Xandi, Toni, Pogi, Joachim, Lisa (und noch viele mehr) – ohne euch wäre mein Leben nicht das was es heute ist und ich wäre wahrscheinlich nicht am Abschluss meines Studiums.

Danke!

Abstract

When creating 3D-Raman-maps of samples three problems occur due to refraction at the sample surface: compression of the depth scale, loss of signal and loss of depth resolution. A common way to avoid refraction is the use of oil (with polymers) with a refractive index close to the sample's or water (with biological samples) and immersion objectives. This, however, contaminates the samples and can even damage the sample, for example by dissolution or diffusion into porous samples.

The first part of this thesis introduces four representative samples and shows that depth scale compression of up to 47% occurs in measurements in air compared to the ones in oil. The measurement in air of an ideal sample shows an about 4 times higher loss of signal with depth compared to measurements using immersion oil.

In the second part of this thesis, several approaches to prevent the contamination of samples by oil are introduced. Of these, adhesive tape and a silicone thin film have proven to be most practical and reliable. Both, adhesive tape and a silicone thin film, successfully avoid loss of signal, compression and prevent the oil from contaminating the sample (contamination with glue from the adhesive tape still occurs). In addition, both approaches can easily be implemented for standalone Raman microscopes.

The final part of the thesis explores the possibility to extend the concept of immersion objectives to the up-and-coming field of correlative Raman-SEM-imaging (Scanning Electron Microscope). However, the approaches from the second part cannot be used as the oil is still exposed to the vacuum of the chamber and would evaporate. Therefore, additional approaches were tried with the aim to enclose the immersion oil fully by some protective layer that can also maintain good optical contact to the sample, which proofed to be necessary. The "arc approach" has shown the highest potential. The arc (a transparent, stiff polymer) as the basis holds the oil, is mounted on the objective and provides the necessary downwards-pressure to ensure good optical contact to the sample. To avoid air inclusions or vacuum bubbles the arc's side towards the sample is coated with an adaptive material. The combined setup was unable to perform adequately, however, each part on its own did yield promising results, which suggests that further research could allow for 3D, confocal, refraction free and sample protecting Raman microscopy automatically and under high vacuum conditions.

Kurzfassung

Bei der Erstellung von 3D-Raman-maps von Proben treten aufgrund der Brechung an der Probenoberfläche drei Probleme auf: Kompression der Tiefenskala, Signalverlust und Verlust der Tiefenauflösung. Eine übliche Methode zur Vermeidung der Brechung ist die Verwendung von Öl (bei Polymeren) mit einem Brechungsindex nahe der Probe oder Wasser (bei biologischen Proben) und Eintauchobjektiven. Dies kontaminiert jedoch die Proben und kann sogar die Probe beschädigen, z.B. durch Auflösung oder Diffusion in poröse Proben.

Der erste Teil dieser Arbeit stellt vier repräsentative Proben vor und zeigt, dass bei Messungen in Luft eine Kompression der Tiefenskalen von bis zu 47% im Vergleich zu Messungen in Öl auftritt. Die Messung in Luft einer idealen Probe zeigt einen etwa 4-mal höheren Signalverlust mit der Tiefe im Vergleich zu Messungen mit Immersionsöl.

Im zweiten Teil dieser Arbeit werden mehrere Ansätze zur Verhinderung der Kontamination von Proben durch Öl vorgestellt. Von diesen haben sich Klebeband und ein dünner Silikonfilm als die praktischsten und zuverlässigsten erwiesen. Sowohl Klebeband als auch ein dünner Silikonfilm vermeiden erfolgreich Signalverlust, Kompression und Kontamination der Probe (mit Ausnahme von Klebstoffresten vom Klebeband). Darüber hinaus können beide Ansätze leicht für eigenständige Raman-Mikroskope implementiert werden.

Der letzte Teil der Arbeit untersucht die Möglichkeit, das Konzept der Immersionsobjektive auf den aufstrebenden Bereich der korrelativen Raman-SEM-Mikroskopie auszudehnen. Die Ansätze aus dem zweiten Teil können jedoch nicht verwendet werden, da das Öl noch dem Vakuum der Kammer ausgesetzt ist und verdampfen würde. Daher wurden zusätzliche Ansätze

erforscht, mit dem Ziel, das Immersionsöl vollständig durch eine Schutzschicht zu umschließen, welche allerdings auch einen guten optischen Kontakt zur Probe aufrechterhalten kann. Der "Arc-Ansatz" gezeigte das höchste Potenzial. Der Arc – ein transparentes, steifes Material dient als Basis, welche das das Öl hält – wird in einem Bogen unter das Objektiv montiert und sorgt durch die Krümmung für den notwendigen Abwärtsdruck, um einen guten optischen Kontakt zur Probe zu gewährleisten. Zur Probe hin ist am Arc ein adaptives Material aufgebracht, um Lufteinschlüsse oder Vakuumblasen zu vermeiden. Der kombinierte Aufbau war jedoch nicht in der Lage, ein zufriedenstellendes Ergebnis zu liefern. Jeder Teil des Aufbaus für sich allein allerdings schon, was zu der Annahme führt, dass durch weitere Untersuchungen und Experimente eine automatische und unter Hochvakuumbedingungen stattfindende dreidimensionale, konfokale, brechungsfreie und probenschonende Raman-Mikroskopie ermöglichen könnten.

Content

1 Introduction

Raman scattering or the Raman effect was discovered by Sir Chandrasekhara Venkata Raman, an Indian physicist in liquids and published in 1928 [1]. It describes the inelastic scattering of photons from molecular vibration. The shift of energy of the photons gives information about the molecular composition which makes Raman spectroscopy an important tool for investigations of different kinds of materials and it has many applications in physics, biology, chemistry and medicine.

A Raman microscope combines the molecular sensitivity of Raman spectroscopy with the spatial resolution of an optical microscope, which makes it possible to create a 2D map of the components of a sample. This is done by measuring and evaluating a Raman spectrum in every pixel of the map [2], [3]. The scanning confocal laser Raman microscope used in this study allows for 2D mappings of the surface as well as depth profiles and 3D mappings of the sample [4]. Depending on the used laser, pinhole and few other parameters, confocal Raman microscopy has a very high spatial resolution with lateral resolutions as low as 200 nm and a depth resolution as low as 500 nm [4].

A problem that specifically occurs with 3D-measurements and depth profiles is refraction, as the materials to be investigated have a significantly larger refractive index than the material between objective and the sample (air in the standard setup; $n_{air} < 1.0003$). Based on Snellius' law, this difference leads to refraction at the sample surface and therefore compression of the depth scale and loss of both resolution and signal [5]. Many samples such as polymers as well as the samples investigated in this study have a refractive index in the range of $n_{sample} \approx 1.3 - 1.6$ [6].

One approach to avoid the occurring information loss through refraction in 3D confocal Raman spectroscopy is the usage of oil as filling material [7]. The hence needed oil immersion objective is immersed into the oil, which must have a refractive index similar to one of the samples to be examined (for polymers around 1.5; for biological samples, water is often used [8]). Hence, the sample must have certain properties such as a sealed surface to prevent absorption and it must not dissolve in oil. Additionally, the sample will be contaminated with oil, which in some cases must be avoided. An approach based on introducing a protective layer between the sample and the oil, to overcome these limitations, has

been suggested in the literature [9]. Expanding on this idea, in this thesis new approaches were developed and evaluated, some of which enable contamination-free, immersion, confocal Raman spectroscopy. A special focus was also put on trying to develop a setup that could ensure the necessary “refractive” contact as well as completely enclose the immersion oil. This would be a rather useful tool in the relatively new field of correlative Raman-SEM microscopy [4], [10], [11], allowing immersion microscopy in the vacuum of an SEM chamber.

A variety of approaches have been tested, three of which yielded useable results. First, the unsuccessful attempts are explained briefly. After that, the three solutions that worked adequately are discussed in more detail. The simplest solution found, was to use customary adhesive tape to shield the sample from the oil. This does not temper with the Raman signal but of course, leads to contamination of the sample with glue. To avoid the contamination with glue, a self-adhesive silicone thin film was tried, which eliminated the contamination problem, but still is not suitable for vacuum applications. The most complex approach using a self-made device to hold a multi-layer foil (the top layer of which is the silicon adhesive), was developed and proof of principle could be accomplished. This third approach could potentially be included in an oil immersion objective, potentially allowing for both more convenient measurements and even use in vacuum.

2 Basics

2.1 Raman spectroscopy

When photons hit a molecule, they are absorbed by it, elevating it to a virtual state. The exited molecule goes back to its ground state emitting a photon with the same energy. This is elastic scattering or Rayleigh scattering [3] and is visualized in Figure 2.1.

In 1923, the Austrian theoretical physicist Adolf Smekal predicted inelastic scattering of light. The paper of Indian physicist Sir Chandrasekhara Venkata Raman (7 November 1888 – 21 November 1970) ”Molecular Diffraction of Light” [1] describes this effect in liquids and it was named after Raman (sometimes Smekal-Raman effect). Independently discovered and published was the effect for crystals by Grigory Landsberg and Leonid Mandelstam [12].

Inelastic scattering can happen in two ways. If the molecule absorbing a photon was already in an excited state it will drop back to its ground state, releasing a photon with its incident energy plus the energy difference between the ground state and the excited state of the molecule. This is called Anti-Stokes scattering (Figure 2.1). The Stokes scattering (Figure 2.1) occurs when a molecule in its ground state is excited from an inbound photon and drops down to a state above the ground state. The exiting photon then gains the energy difference between the molecules ground and final excited state. As it is more likely that molecules are in their ground state, Stokes scattering occurs more often and is used for Raman spectroscopy [1], [3], [12].

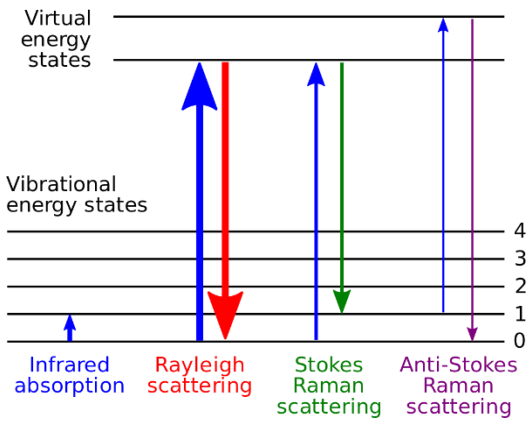

Figure 2.1: Representation of Rayleigh, Stokes Raman and Anti-Stokes Raman scattering.

In classical physics, Raman scattering is explained through polarization [2], [13], [14]. Photons can excite molecules to a virtual energy state by producing an oscillating polarization. These polarizations can couple with other possible polarizations of the molecules. The number of possible polarizations is mainly limited by the degrees of freedom and electronic excitations. The degrees of freedom are given by $3N - 5$ in linear molecules and $3N - 6$ in non-linear molecules, where N is the number of atoms in the molecule [15]. Elastic scattering occurs, when the polarization in the molecule, caused by the incident photon, does not couple with these possible polarizations; the scattered photon will have the same frequency, wavelength and therefore energy as the photon entering the compound. If the polarization in the molecule couples with another polarization, the scattered photon differs in energy by the amount required to excite the molecule. This difference can be positive or negative. If the material observed absorbs energy from the incoming photon, the scattered photon will have lost energy and undergone the already introduced Stokes Raman scattering. In the opposite case, when the scattered photon has gained energy (and therefore the material has lost energy), the scattering event is called anti-Stokes Raman scattering. The scattered photons can be collected and analysed to become a Raman spectrum.

Approximately only 1 out of 10 million photons are scattered inelastically [16]. Therefore, in Raman spectroscopy, a laser is used to excite molecules. The elastically (Rayleigh) scattered photons are blocked by a filter and inelastically (Raman) scattered Photons are measured by a spectrometer equipped with a highly sensitive photon detector. An example of a Raman spectrum can be seen in Figure 2.2 where Polyethylene was sampled.

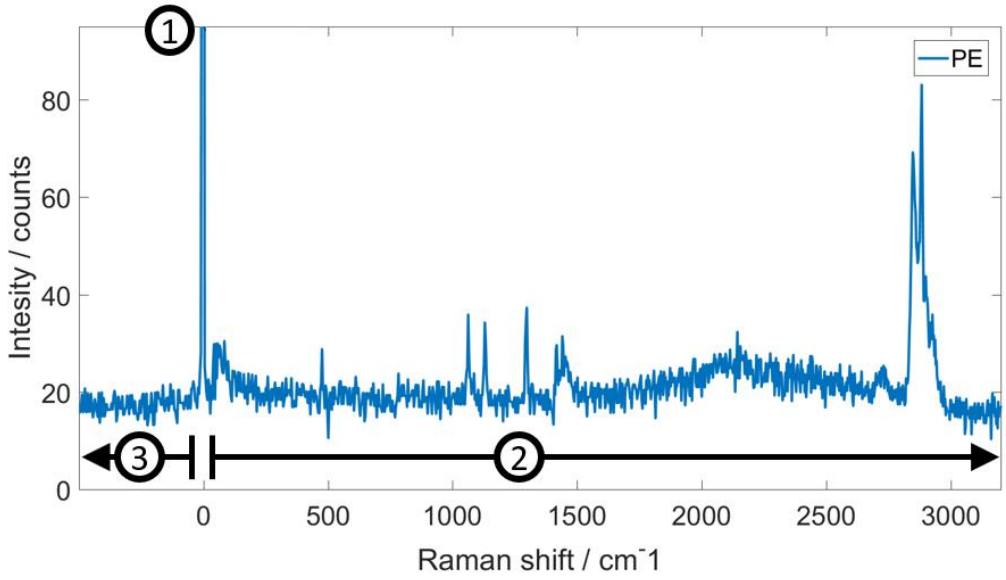

Figure 2.2: Example of a Raman spectrum of Polyethylene:

(1) elastically scattered photons from the laser
(2) inelastically scattered photons - undergone Stokes Raman shift
(3) inelastically scattered photons - undergone Anti-Stokes Raman shift.

General settings can be seen in 9.2.

Settings specific to this measurement:
Laser intensity: 100%
Integration time: 1 sec

The peak at position 1 in Figure 2.2 represents the elastically scattered photons that did not lose energy. The inelastically scattered photons in area 2 have lost energy and have undergone a Stokes shift, where the energy was given to the observed material Polyethylene. In area 3 the photons have gained energy, taking it from the sample and have undergone an Anti-Stokes shift (Note that this spectrum was measured with a low-pass filter thus no Anti-Stokes photons can be detected; the occurring counts come from background noise). The amount of energy the photons lost or gained is directly proportional to the indicated inverse length unit: the wavenumber. The recorded spectra contain a lot of information about the sample such as chemical composition, the stress/strain stated, crystal symmetries and crystal quality [3], [17].

2.2 Raman microscopy

A Raman microscope uses a monochromatic and polarized light source, usually a Laser, which is focused on a small area on the sample. After scattering, the photons are collected with a lens (most commonly backscattered through the microscope objective) and send through a Raman spectrometer. An additional pinhole in a confocal setup limits the scattering volume in the z-direction.

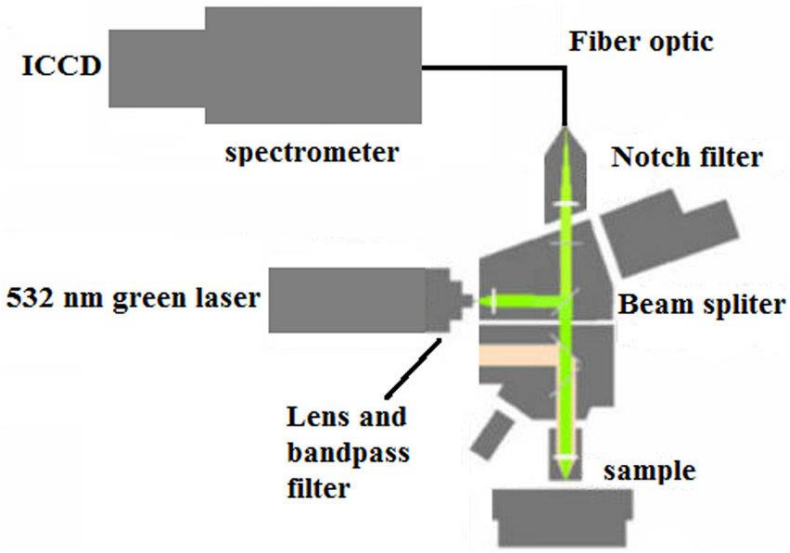

Figure 2.3: Sketch of a Raman microscope setup. Credit: [18]

A sketch of this setup is shown in Figure 2.3 for clarity. The actual Raman microscope (The LABRAM HR 800) used for this thesis is introduces in chapter 9.1 and can be seen in Figure 9.1 . With a Raman microscope setup like this, it is possible to measure Raman point spectra with microscopic resolution, by scanning the laser (analogue to a confocal scanning microscope) mappings become possible [7].

2.3 Mapping

Images of light microscopes are taken by a camera. A spectral mapping is done by scanning over the sample pixel by pixel, measuring one spectrum per pixel. The analysing software gives a colour code for chemical compounds and draws or overlays a colour map, as illustrated in Figure 2.4. This is done by either univariate methods (such as band integration or band fits) or multivariate methods (such as CLS, PCS) [19].

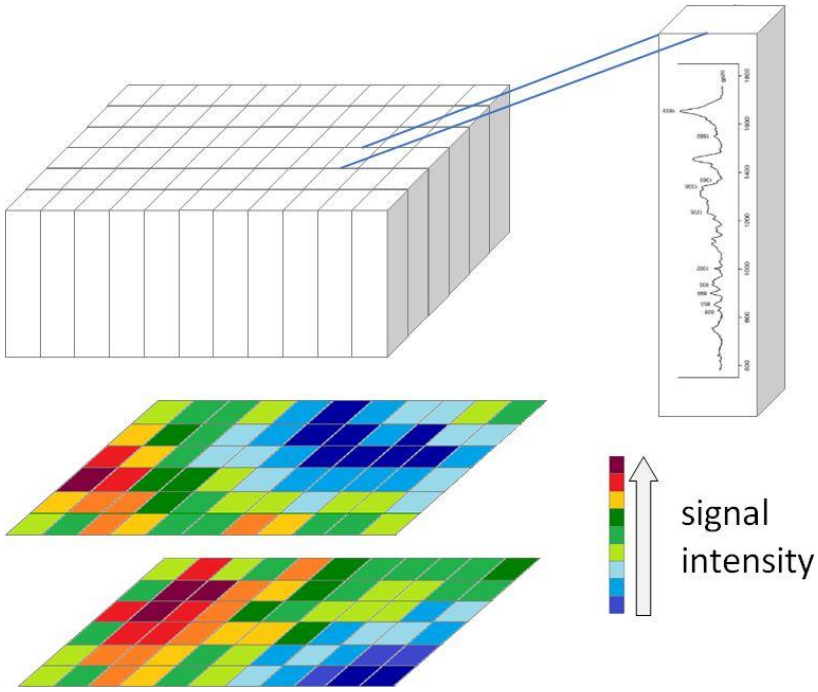

Figure 2.4: Visualization of how spectral images are created.

The scanning area does not have to be restricted to the surface. Samples transparent to the chosen wavelength of the laser can be measured in three dimensions. With the right settings, voxels of the size of 1 µm in each direction can be recorded. If the sampled specimen has a refractive index much greater than 1 (which is usually the case) refraction will occur [5], [7], [20], [21].

2.4 Refraction

Refraction occurs when a wave changes the medium it is transmitted in and is described by Snell's Law. The mathematical form is

$$\frac{\sin\theta_1}{\sin\theta_2} = \frac{n_2}{n_1} \qquad (1)$$

where θ_1 is the angle of incidence, θ_2 the angle of refraction and $\frac{n_2}{n_1}$ is the ration of relative indices of refraction of the two media where the transition takes place. It describes that a wave with a single frequency will change the direction of propagation depending on the angle of incident and refractive indices of the media participating. A sketch of this phenomenon can be seen in Figure 2.5 . This is due to conservation of energy and momentum which means, that the frequency must not change. However, due to the change of medium, the phase velocity changes and with it the direction of propagation [22].

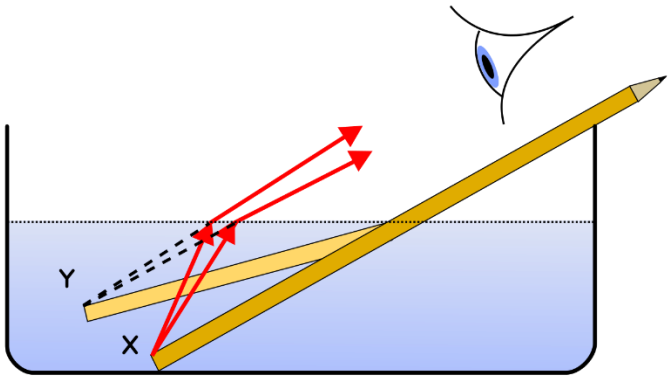

Figure 2.5: Schematics of optical refraction. Image source: Wikipedia (CC).

In case of measurements beneath the surface of a sample, like in 3D-maps of Raman microscopy, the point of origin of most of the Raman shifted photons is at a deeper distance, than the software is calculating with. In Figure 2.6 the dashed line represents the optical path neglecting refraction. Due to a higher refractive index in the sample, the photons are focused on a deeper point into the sample (solid line). The analysing software, however, calculates with coordinates above the actual point, the point where the photons would focus if no refraction had occurred. Therefore, depth information is compressed which has been shown extensively in several papers by Everall [5], [7], [20], [21].

Additionally, resolution and intensity are decreased, sometimes to a point where no useful information can be obtained [5], [7], [20], [21]. This can be avoided by filling the gap above the specimen with a substance, that has a refractive index in the range of the sample [20]. For samples with a refractive index around n ≈ 1,3 like biological samples, water is used to decrease refraction losses. For samples with a refractive index in the area of $n \approx 1.5$ like polymers, immersion oil is used. In any case, an immersion objective specially designed for its intended use must be used.

When using immersion objectives and an immersion liquid refraction can be reduced, ideally neglected. However, when using a liquid to fill the gap consequences emerge. The contact of sample and liquid contaminates the sample, which in some cases, must be avoided. Additionally, when specimen are porous or absorptive measurements cannot be conducted as the liquid would trickle away and could no longer serve for its intended purpose. Another occurring effect is the upwards oriented pull caused by the surface tension of the liquid.

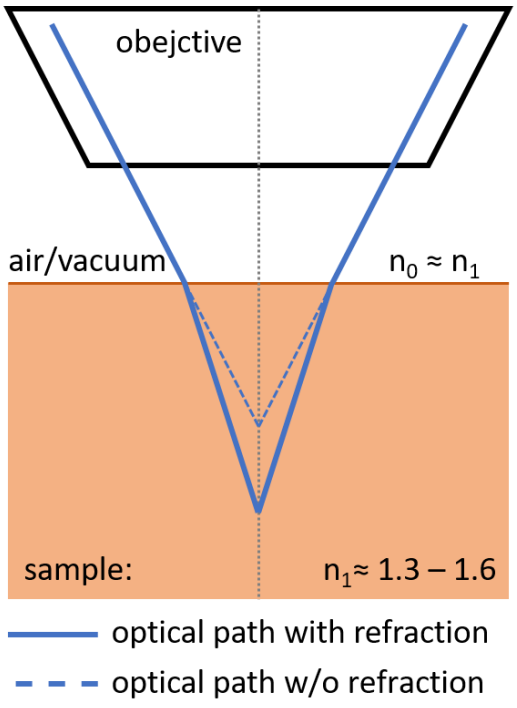

Figure 2.6: The optical path of the light beam emerging from the objective through air or vacuum into the sample with a refractive index $n_1 \approx 1.3 - 1.6$.

Several methods have been tried where an additional layer is introduced to protect samples from immersion liquids [9]. The layer must have a refractive index in the range of the sample. With now two phase transitions an additional source of possible information loss is created, however, if the refractive indices of the sample, protective layer and immersion liquid match, the losses are small enough to be neglected. Another crucial point is that there must be good contact between the protective layer and the sample, which in [9] is realized by putting the sample in a small vacuum apparatus with the protective layer on the top side as seen in Figure 2.7 where the light blue line is the protective layer containing a low vacuum.

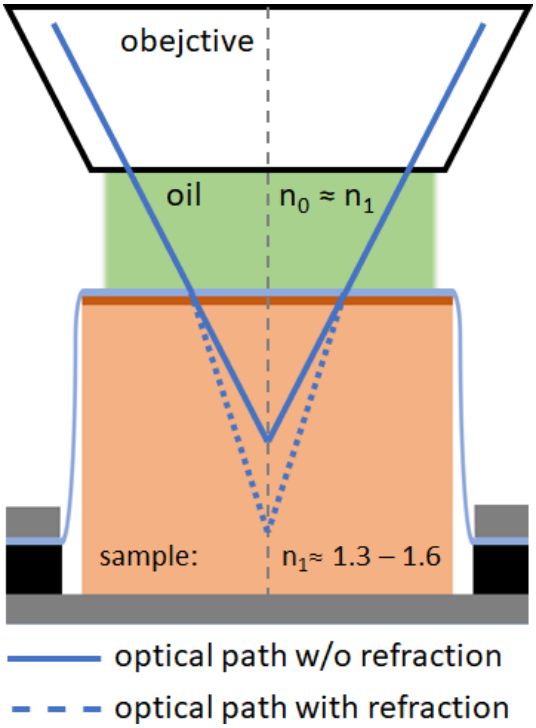

Figure 2.7: Representation of the experimental setup of [9] used to reversibly apply a protective film (light blue line).

The protective layer prevents contact of the sample with the immersion liquid, however, in the relatively new field of correlative Raman SEM microscopy there is an additional problem. The vacuum in the SEM chamber will evaporate the immersion liquid. In this application, it is thus necessary to find an approach that fully encloses the oil and is vacuum stable, while still maintain good contact between the sample and protective layer.

3 Samples

Introduced in this chapter are the four mainly used samples in this study. Each sample is introduced separately, its advantages and disadvantages are listed and representative Raman spectra of the relevant components of each are shown as well. A short visual introduction can be seen in Figure 3.1.

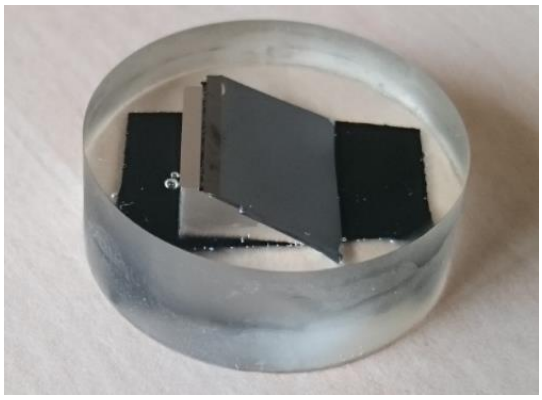

(a) Silicon waver embedded at 45◦ angle; no surface abrasion.

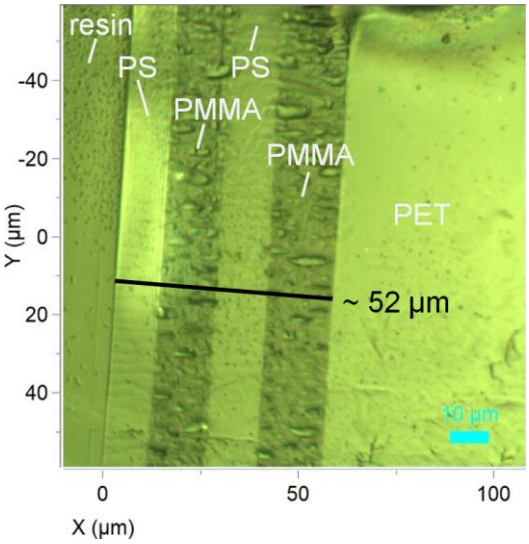

(b) Cross-section of the Polymer-Multilayer-foil consisting of different polymers on a PET carrier Foil. Thickness about 52 µm

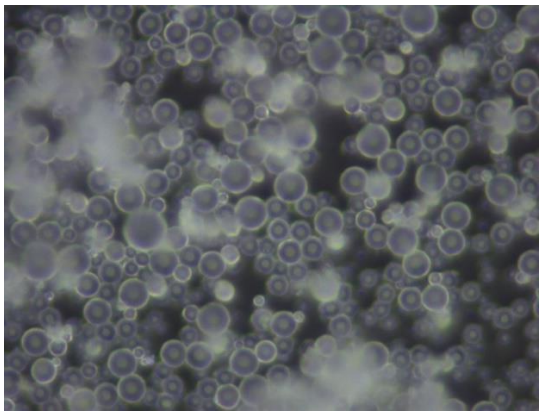

(c) Poly(styrene-co-divinylbenzene) beads. Average size 8-9 µm.

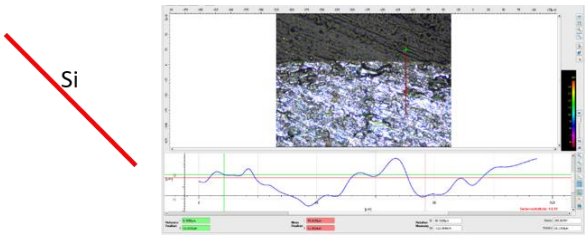

(d) Silicon waver, embedded at 45◦ angle, surface abrasion fabricated with sandpaper (smallest grain size 10 µm)

Figure 3.1: The Four mainly used samples.

3.1 Si45 – Silicon waver embedded at 45° degrees

Silicon has a strong and clear Raman signal, which can be seen in Figure 3.2. A clean, polished silicon waver was taped on a carrier piece of metal, embedded, sanded and polished, so both the metal and the silicon are accessible on the clean and polished surface. In Figure 3.1 (a) the sample (from now on referred to as Si45) can be seen with the metal piece embedded at a 45° angle to the surface. Its geometry predicts, that for every distance on the surface away from the edge, the silicon signal must be detected in the same distance beneath the surface. Otherwise, refraction and therefore compression has occurred. The specimen is robust and reproduced fast and easily. A downside of the Si45 is, that it does not represent realistic samples, as such are often fragile and usually return little signal.

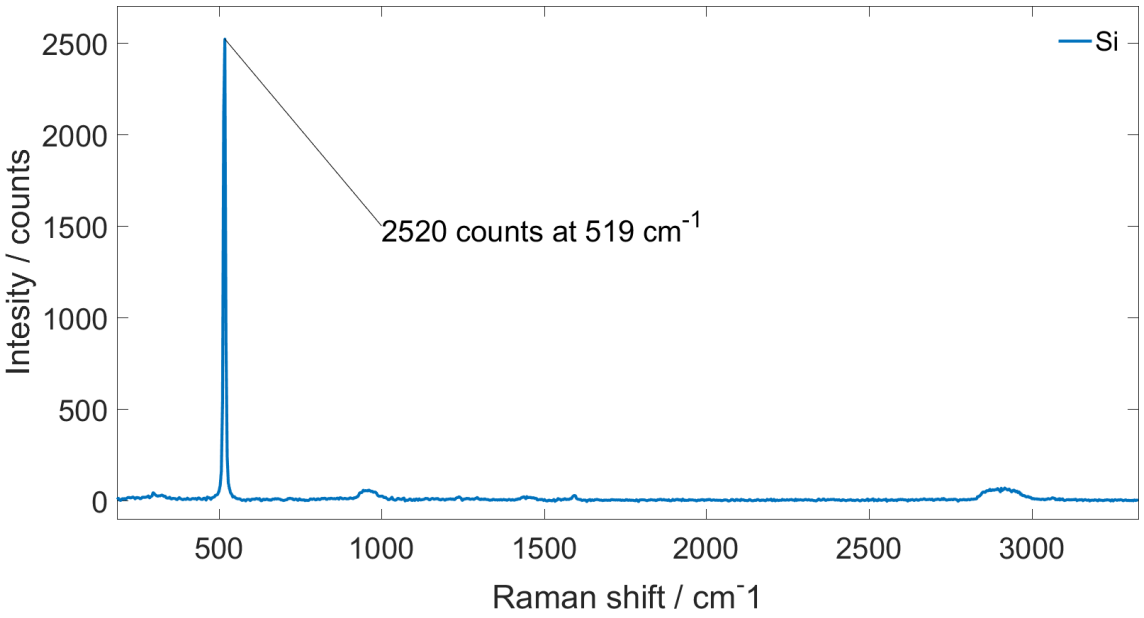

Figure 3.2: Raman Signal of Silicon. Literature value: 520 cm-1 [23].The small bands are higher order vibrations and due to the embedding resin.

Settings:	*Laser intensity:*	*100%*
	Integration time:	*0,02 sec*

3.2 PMLF – Polymer-Multi-Layer-Foil

To simulate more realistic samples a polymer-multi-layer-foil was produced. Its cross-section is displayed in Figure 3.1 (b). The Raman spectra of the different materials used as well as a representation are displayed in Figure 3.3. On a PET (5) carrier foil four layers of (1) polymethylmethacrylate (PMMA), (2) polystyrene (PS), (3) PMMA, (4) PS were successively liquefied in a solution, applied with a doctor blade and dried. This polymer-multi-layer-foil (from now on referred to as PMLF) has a total thickness of about 52 µm from the beginning of (1) until the end of (4). PMLF represents samples which are commonly analysed in industry applications, where parameters of interest could be thickness, composition and transition properties. The downside of this sample is its 2D restriction. Strictly speaking a 1D scan in z-direction is enough to learn its architecture and detect possible compression, however, a 2D-scan is more representative and can show slight irregularities in the total or single thickness of the layers.

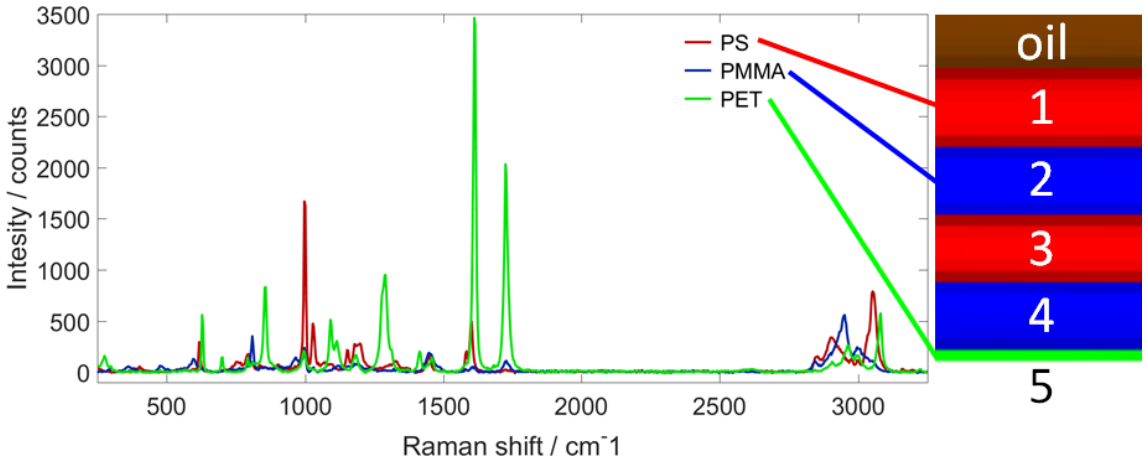

Figure 3.3: Raman Signal of PET, PMMA and PS.

Settings: Laser intensity: 50%
Integration time: 0,5 sec

3.3 PSuB – Poly(styrene-co-divinylbenzene) micrometer Beads

To truly have a 3D structure a sample was manufactured. This sample should have geometries with defined sizes. They must be larger than the minimal resolution of the used Raman microscope of about 1 µm and smaller than about 15-20 µm to have at least one full view in the obtained 2D and 3D images.

The company Aldrich[1] provides industrially manufactured beads of Polystyrene-co-divinylbenzene, with an average size of about 8-9 µm as seen in Figure 3.1 (c) where the beads were imaged with an infinite focus microscope. These beads were embedded in epoxy resin[2] like in Figure 3.4 (a) and slices of about 15 µm were cut with a diamond knife using an Ultramicrotome Laica. The slices, also seen in Figure 3.4 (a) must be handled with care but pasted on adhesive tape handling is simplified. An SEM image of the PSuB-sample - not embedded - can be seen in Figure 3.4 (b). The beads vary in size between about 1-20 µm ideal for a test sample for 3D-Raman-mappings.

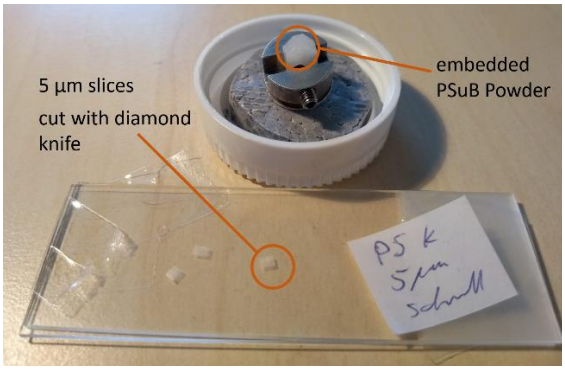

(a) Embedded PSuB powder and diamond knife cut, 5 µm slices on a glass substrate.

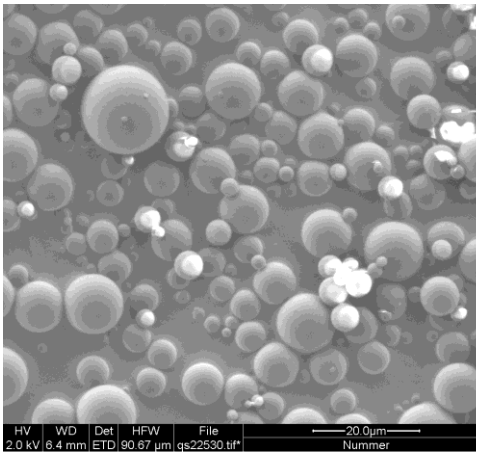

(b) SEM image of the PSuB sample – not embedded.

Figure 3.4: Prepared PSuB and SEM image

[1] www.sigmaaldrich.com
[2] Spezifix 40, www.struers.com

These polystyrene micrometer beads (from now on referred to as PSuB) represent a realistic sample with 3D structures underneath the surface. The spectrum of the beads can be seen in Figure 3.5. The downside of this sample is its complex preparation and fragility.

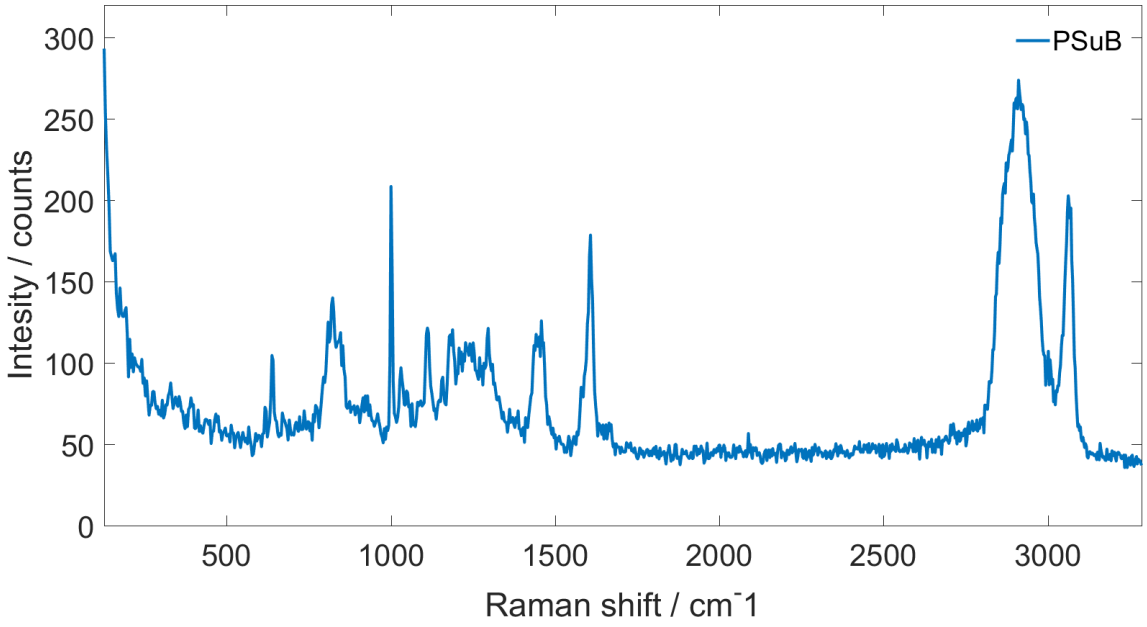

Figure 3.5: Raman spectrum of the PSuB.

Settings: Laser intensity: 25%
Integration time: 1 sec

3.4 Si45-abr – Silicon waver embedded at 45° degrees with abrasive surface

Some samples have an abrasive surface. To simulate such samples the sanding procedure of a second Si45 sample was halted before the polishing process which results in an abrasive surface. The last sandpaper used had a grain size of about 22 µm. A 2D surface scan executed with an Infinite Focus microscope can be seen in Figure 3.6. It shows that the sample (from now on referred to as Si45-abr) has surface abrasions with height differences of up to 2 µm. The silicon waver embedded at 45° angle allows for immediate information of compression. Its Raman spectrum is the same as the one of Si45 and can be seen in Figure 3.2. The purpose of this sample is to test, if a good contact optical contact can be assured even for rough surfaces.

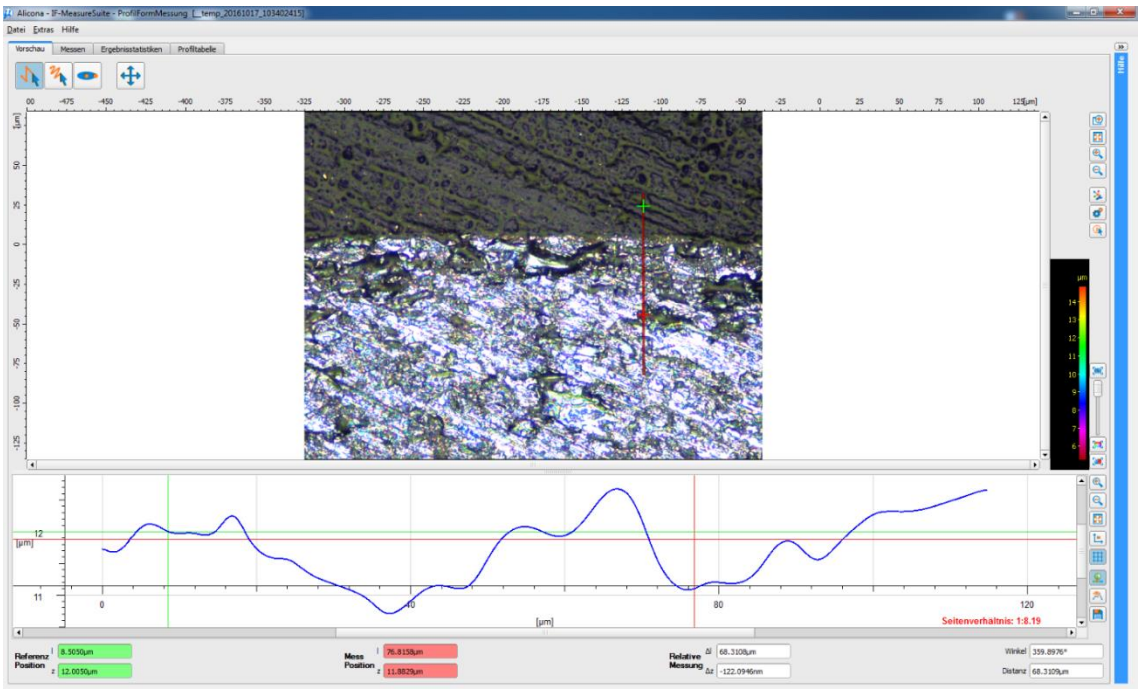

Figure 3.6: Surface scan of Si45-abr along the red line conducted with an infinite focus microscope. Height difference up to 2 µm.

4 Measurements with and without oil-immersion

Due to refraction, spectra beneath the surface appear from a compressed distance. This will be demonstrated in this chapter by displaying measurements of the samples conducted in air and comparing them with the method of using immersion oil. Additionally, the measurements in this chapter serve as a benchmark for all approaches tested.

The most commonly used way to avoid refraction is to fill the space above the sample with a drop of immersion oil ($n_{oil} \approx n_{sample}$) on the spot to be examined and immersing an immersion objective in it. This reduces the difference in refractive indices to a level, where the occurring compression is minimal. The used immersion oil for this study is from the company Reichert in Vienna. The refractive index of $n_D = 1{,}516$ is within the range of the examined samples and reduces refraction so it can be ignored, as is demonstrated by the example of the Si45 sample.

4.1 Si45

The most conclusive visualization of compression can be observed with the silicon waver embedded at a 45° angle where compression directly shows in the angle of the detected silicon surface. The left image in Figure 4.1 was taken with oil to avoid refraction and therefore compression should not occur. It is evident that the silicon waver is indeed detected at a 45° angle: 60 µm away from the edge the signal is detected at the same distance, 60 µm into the sample.

The right image in the same figure shows the result obtained without oil in the gap which results in the optical path being refracted and giving a compressed signal. The expected signal of silicon in 60 µm, 60 µm away from the edge is hardly detected at a depth of about 30 µm below the flat surface, which gives a compression of about 47%. Additionally, the signal over depth drops with a more than three times higher rate than when measured directly with oil. These results agree with the calculation/demonstrations by Evrall [21].

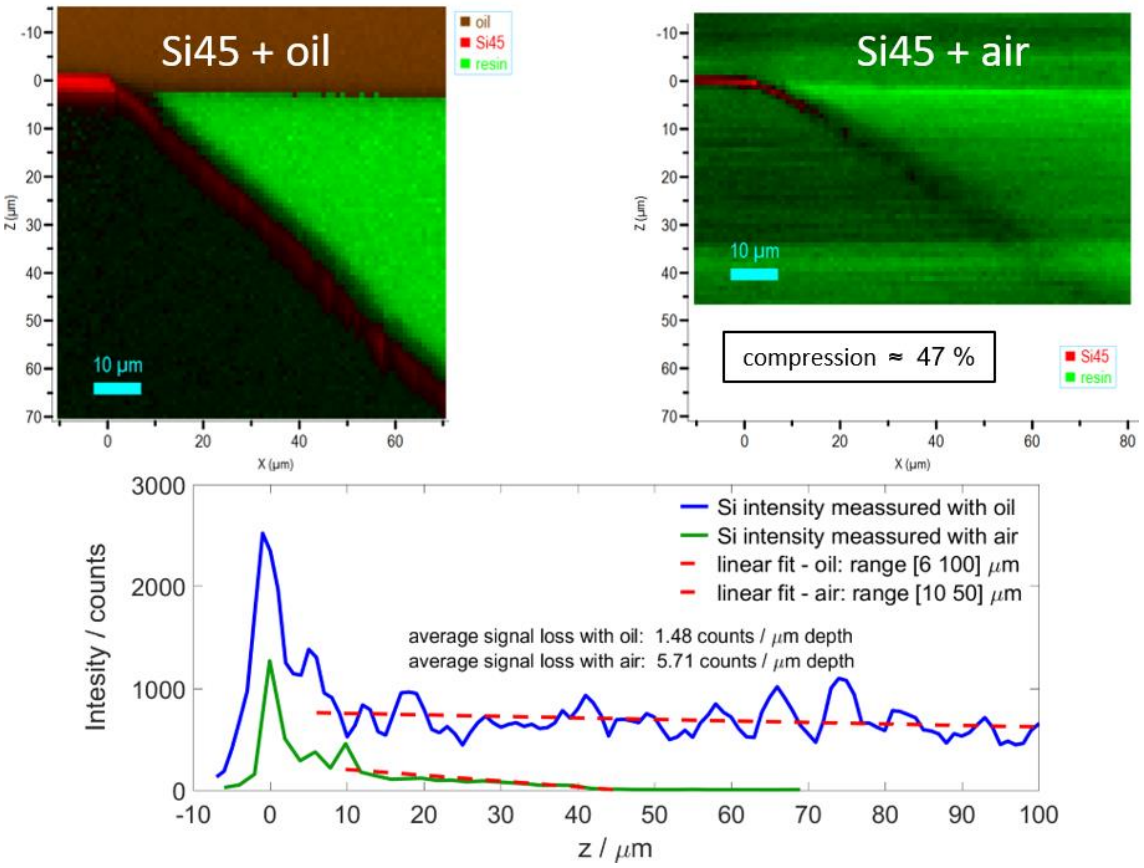

Figure 4.1: Signal of the embedded Si45

The top two images show the 2D-scan of the Si45 sample measured with (left) and without oil (right) as refraction prevention.

The image at the bottom shows the intensity of the silicon signal over depth, measured with (blue line) and without oil (green line). The dashed red line is a linear fit over a given range to determine the average signal loss over depth.

4.2 PMLF

The polymer-multi-layer-foil is also a very clear representation of the occurring compression. The two results, obtained with and without oil to prevent refraction, are displayed at the top in Figure 4.2. The top two images use the same scale and show the three materials used in the composition: PS, PMMA and PET.

The image at the bottom shows the intensity of the materials in this composition over depth. For these graphs, the corresponding 2D map of PMLF (top image) was averaged over each row and normalized to the maximum of each material, for clarity.

The 2D maps clearly display the occurring compression due to the absence of oil. The thickness of each individual layers, as well as the total thickness, are compressed in the map measured without oil. The thickness obtained with the measurement without oil, at air is less than 30 µm which results in a compression of more than 40%. This is confirmed by the bottom image of Figure 4.2 where the signal loss of PS and PMMA from the first to the second occurrence is significantly larger in the measurement with oil than without oil. Also, the position of each peak is closer to the surface at z = 0 which is evidence of compression. Additionally, the smearing of the transitions between the lower layers visible in the bottom of Figure 4.2, is evidence of a loss of resolution.

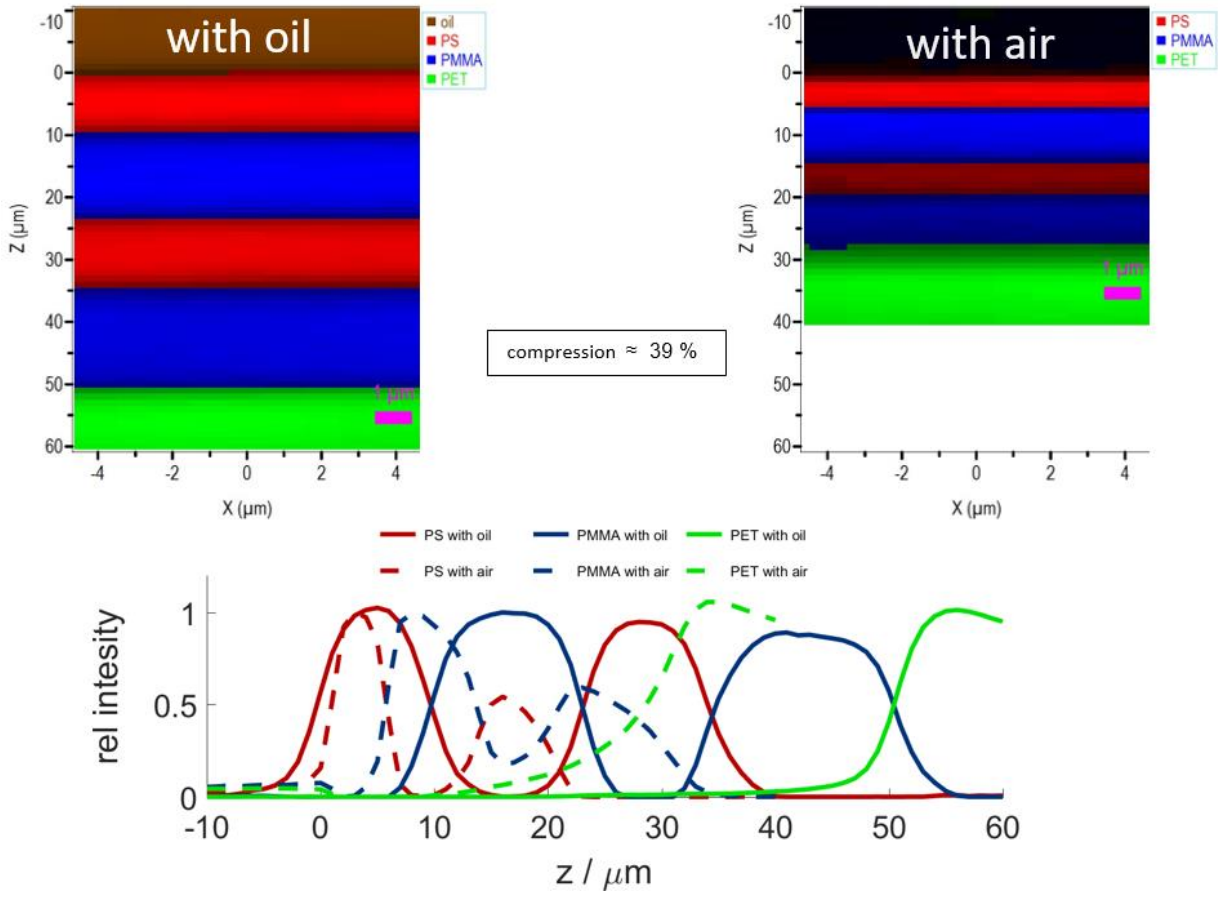

Figure 4.2: Signal of the PMLF.

The top two images show the 2D-scan of the PMLF sample measured with (left) and without oil (right) as refraction prevention.

Settings:	*Laser intensity:*	*25%*
	Integration time:	*1 sec*

Admittedly each layer of the PMLF has a different refractive index and therefore each transition results in refraction, which could be an additional source for occurring compression. The fact that measurement with oil yield spectra with hardly any signal loss or compression over depth contradicts this. Additionally, the differences in the refractive indices of the materials are very little and can, therefore, be neglected. The literature refractive indices[3] are listed below:

- Polystyrol (PS): $n_{PS} = 1.5916$
- Polymethylmethacrylat (PMMA): $n_{PMMA} = 1.5916$
- Polyethylenterephthalat (PET): $n_{PET} = 1.5750$

[3] https://refractiveindex.info

4.3 PSuB

The PSuB represent a realistic and three-dimensional sample. Measurements were conducted with a Laser intensity of 25% to avoid possible burning of the sample caused by the laser. To compensate for the resulting lower signal, the acquisition time was increased to 1 sec per spectrum to obtain a clear signal, distinguishable from the background noise, even in great depths. To display several different beads and their variation in size and depth a large volume had to be measured. A cubic grid of width sizes of 40 µm in each horizontal direction and 50 µm in the z-direction was chosen. With a step size of 1 µm in each direction, with the given acquisition time and two accumulations per spectrum the total time to conduct the measurement added up to about 48 hours. With the finding of previous measurements and limited time available on the measurement instruments, it was decided to conduct measurements on the PSuB-sample with oil only, as further complications and therefore an even longer measurement time due to the loss of signal, resolution and depth compression is expected. Also, a best-case benchmark seemed sufficient for this sample. The 3D representation of the results with oil can be seen in Figure 4.3 where the three-dimensional structure is evident. Only the data from the embedded beads is visualized. Their raw data was interpolated to better visualize the round shape. Together with the optical images in Figure 3.1 & Figure 3.4 the shape and size distribution of the beads can be confirmed.

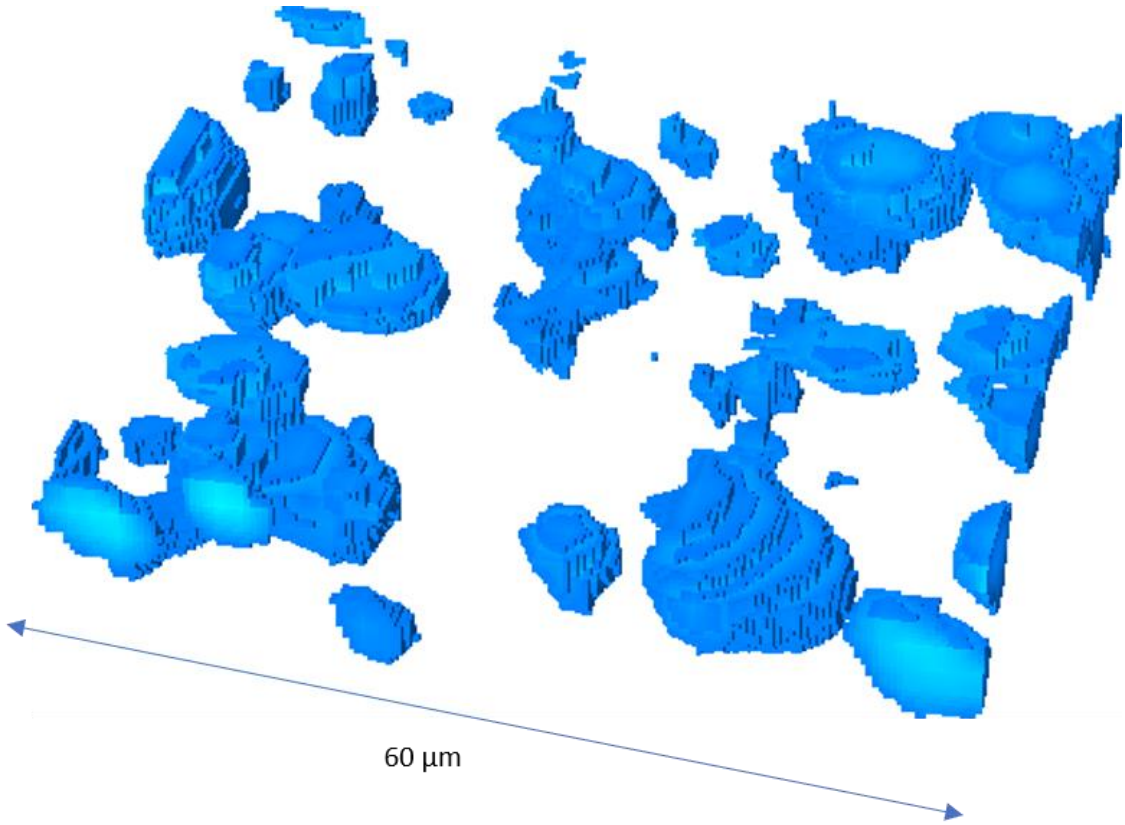

Figure 4.3: 3D image of the PSuB.

Settings: Laser intensity: 25%
Integration time: 1 sec

4.4 Si45-abr

The Si45-sample (without abrasive surface) in Figure 4.4 shows clear spectra, even in depth of 100 µm. The measurements of the Si45-abr-sample, however, yielded usable data only, when measured with oil as a filling material. The corresponding image can be seen in Figure 4.4, where the calculated compression is about 7% which is within a reasonable error range.

Due to the inability to obtain data with this sample measured in air, it was concluded, that the abrasive surface greatly complicates refraction and reflection on the surface, therefore reducing the useable signal to a point that renders mappings practically impossible. This also means that this sample is a particularly interesting test case for all tested approaches.

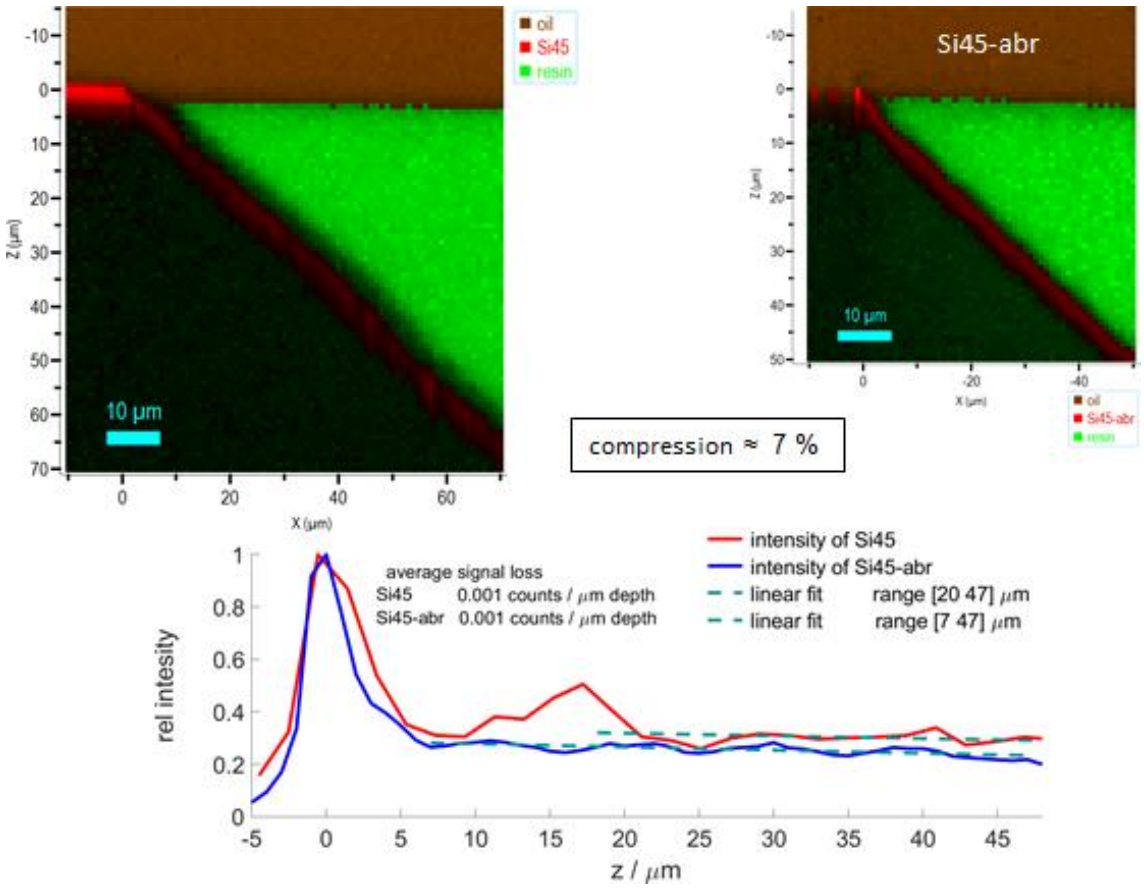

Figure 4.4: Signal of the sample Si45-abr compared to Si45.

Top left image shows the measurement of the SI45.
Top right image shows the measurement of the SI45-abr sample.
Bottom image shows relative intensity over depth of each measurement.

Settings: Laser intensity: 25%
Integration time: 1 sec

5 Oil-contamination-free approaches

In the previous chapter, it could be concluded, that it is necessary to prevent compression and some benchmarks for the main samples have been set. So far this has been done with immersion oil. When using oil, the problem of refraction can be minimized but with its introduction, other problematic factors occur, such as contamination or even damage of the sample. In this chapter, all the approaches, both successful and unsuccessful, are discussed, but first, some fundamental requirements need to be introduced.

Firstly, the surface tension of the oil results in an upward oriented force lifting any sample or setup that is not heavy enough to withstand this force or is not fixated to the table of the microscope sufficiently. This means that in normal immersion microscopy the sample must be fixated somehow, but also that any setup for contamination-free immersion must either exert a downwards force or have enough adhesion to the sample surface. If this is not or not sufficiently the case, then there will be no good contact between the setup and the sample surface and thus refraction will occur.

As explained earlier, an introduced protective layer must have a refractive index similar to the sample's index and must be highly transparent to avoid loss of intensity. Additionally, any used immersion objective has a given working distance d_w and can obtain a signal from depths of distances up to d_w deep into the sample. The additional layer with thickness d_l reduces this available distance of measurement in the z-direction. With thinner protective layers more examinable space is available. Alternatively, an objective with a larger working distance can be used. The objective used in this study had a working distance of $d_w = 200\,\mu m$, therefore any setup must be under 200 µm of thickness.

These conditions are essential to any measurement of this thesis. An overview of how the subsequently introduced methods performed can be seen in Table 5.1, with essential conditions marked in orange. Conditions met are marked with an ✓, conditions not met are unmarked, unchecked conditions are marked with **?** and conditions that, in the eyes of the author, are potentially accomplishable are marked with ~.

Table 5.1: Essential and optional conditions for protective layers.

' '	...	*condition not met*
✓	...	*condition met*
?	...	*condition not checked*
~	...	*condition potentially accomplishable*
l/m/h	...	*subjective surface adaptability low / medium / high*
l/m/h	...	*subjective practicability low / medium / high*

		approach											
condition		PE foil	adhesive tape	silicone foil	box	wax	gelatine	oil sphere	bubble	bag	arc		
											plain	silicone	FSB
essential	adhesion		✓	✓	~				~	~	~	~	~
	$n_{app} \approx n_{sampe}$	✓	✓	✓	?	?	?	✓	✓	✓	✓	✓	✓
	thickness < 100 µm	✓	✓	✓	✓	?	?	?	?	✓	✓	✓	✓
optional	contamination free	✓		✓	✓				✓	✓	✓	✓	✓
	removable	✓	~	✓	✓	~	~	~	✓	✓	✓	✓	✓
	vacuum applicable								✓	✓	~	~	~
	surface adaptability		h	h	m	h	h	h	l	l		h	h
	practicability	l	h	h	m	l	l	l	l	l	m	m	m

Listed in the same table, marked in blue, are optional conditions improving a measurement considering different aspects. Some samples must not be contaminated. An additional layer of any kind will prevent contamination from the immersion liquid, however, the layer itself might contaminate the sample. If a sample must not be contaminated, it usually is to be returned to its origin after examination and therefore, any additional layer must be removable. Considering nowadays more frequently used correlative Raman-SEM microscopy, vacuum applicability was also evaluated. Any approach with loose or evaporable material is unfit for vacuum usage. Some samples have surface abrasions. Taking these into account, the approaches were evaluated in terms of surface adaptability from low (l) through medium (m) to high (h). The additional layers and different approaches present varying additional effort to set up. Listed last is a subjective assessment of each approach's practicability ranging from low (l) through medium (m) to high (h) practicability.

5.1 PE foil

All-purpose PE foil with a thickness of about 7 µm (available in every hardware store) is thin enough to allow decent measurements. It is transparent in the targeted frequencies, impenetrable for oil, does not contaminate samples as it has no additives that could dissolve out, contaminating the sample and it is easily removable. The only essential condition that is difficult to meet is to prevent the PE from being pulled up by the oil. Therefore, the PE foil must be fixated. Attempts to fixate the foil with adhesive tape, outside the optical path have been performed, failing to neglect the presence of air in the optical path.

A workaround was attempted by stretching a large enough piece of the foil on the upside of the glass substrate to avoid wrinkles, fold it to the lower side and twist it, so the foil wraps around the sample on the glass substrate holding it in place and shielding it from oil. An image of a piece of PMLF-sample with the PE foil wrapped around can be seen in Figure 5.1. This approach, however, failed to achieve good contact consistently and/or for a long enough time for meaningful measurements.

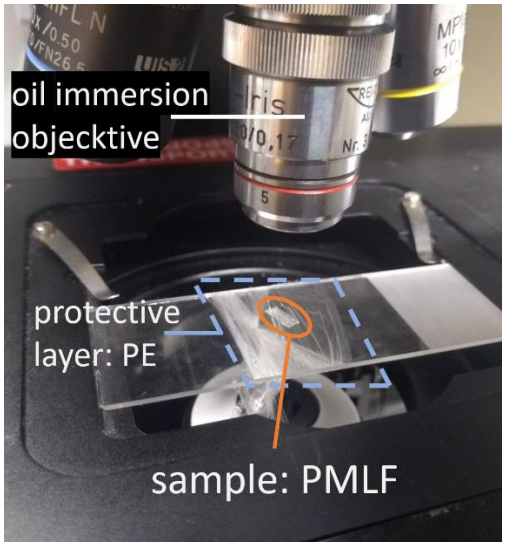

Figure 5.1: Customary PE all-purpose foil used to protect a sample of PET.

To test if the PE foil is potentially applicable (transmission and refractive index), it was taped to a glass substrate with double adhesive tape to receive a setup consisting of glass, glue, carrier foil of the adhesive tape, glue, PE foil and then oil from bottom to top. The results can be seen in Figure 5.2 where the intensity of each material's signal

is displayed over depth relative to its maximum. One can see, that with the chosen settings of measurement the signal in depths greater than about 30 µm decreases in intensity. The task was to verify if a PE foil could be used to protect a layer from oil, which, if applied thoroughly, can be confirmed, as the signal beneath is clearly obtainable. The practicality was assessed to be low as attaching the foil without air inclusions proofed to be cumbersome and the upwards pull of the oil prove impossible to be overcome consistently. This, however, let to the conclusion that a thin layer sticking to the sample would be a simple and reliable approach. Therefore, adhesive tape was tested next.

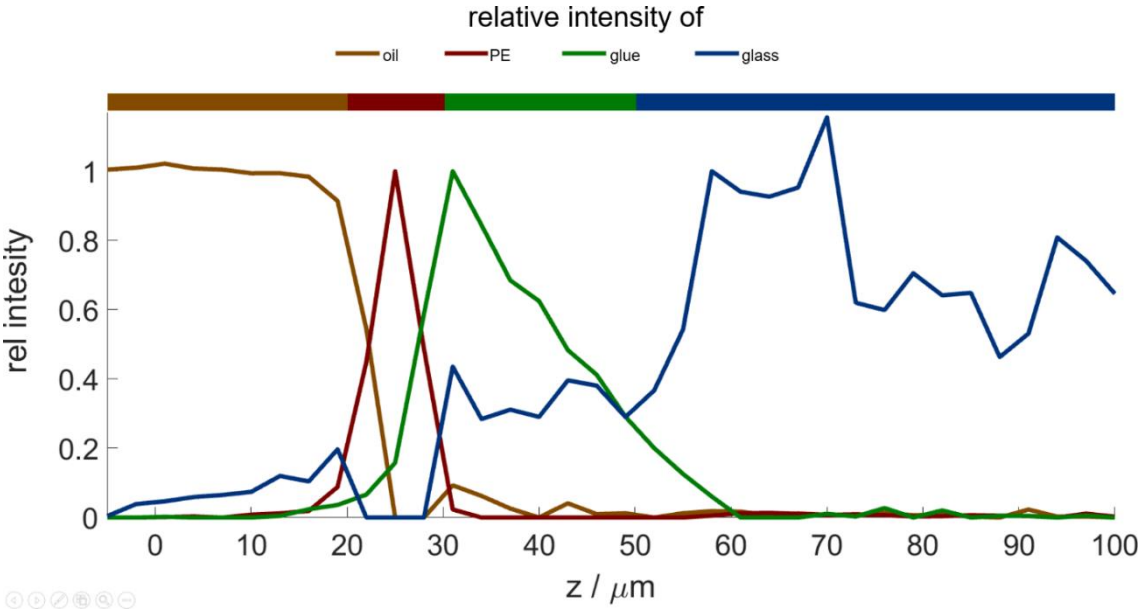

Figure 5.2: Intensity of the Raman signal of all parts of PE on double adhesive tape relative to the maximum of counts of each part. The top bar indicated the thickness and area where each part should be.

Settings: Laser intensity: 25%
Integration time: 1 sec

5.2 Adhesive tape

Customary adhesive tape usually consists of a carrier layer on top of a layer of glue was tried successfully next. It is cheap, readily available and highly transparent in the required frequencies. Additionally, with a thickness of 50 µm, it is thin enough so that the used immersion objective with a working distance of about 200 µm can examine samples in depths of up to 150 µm.

The adhesive nature of the tape is useful to hold small samples in place and the carrier layer shields the sample from oil. Preparation is easily done by placing the sample on a glass substrate and fixating it with adhesive tape. Figure 5.3 shows this setup, which must be fixated to the table of the microscope as the surface tension of the drop of oil is strong enough to lift the whole setup including a glass substrate. Fragile samples or samples that must not be contaminated are not suited for preparation with adhesive tape due to its glue. Vacuum applicability is not given as the oil would evaporate. Small surface abrasions in the range of the thickness of the tape can be adapted to with the glue. The results of these measurements are discussed in chapter 6.1. The disadvantage of the approach with adhesive tape is the contamination of any sample with glue. Therefore, other methods have been tried where contamination is avoided. The idea was to find a contamination-free adhesive foil.

Figure 5.3: Customary adhesive tape applied on a glass substrate to hold the sample PMLF in place.

5.3 Silicone thin film

The ideal protective layer is thin, transparent in the desired frequencies, can hold the sample in place without glue or contaminating the sample otherwise, is removable and does not need long or complex preparation.

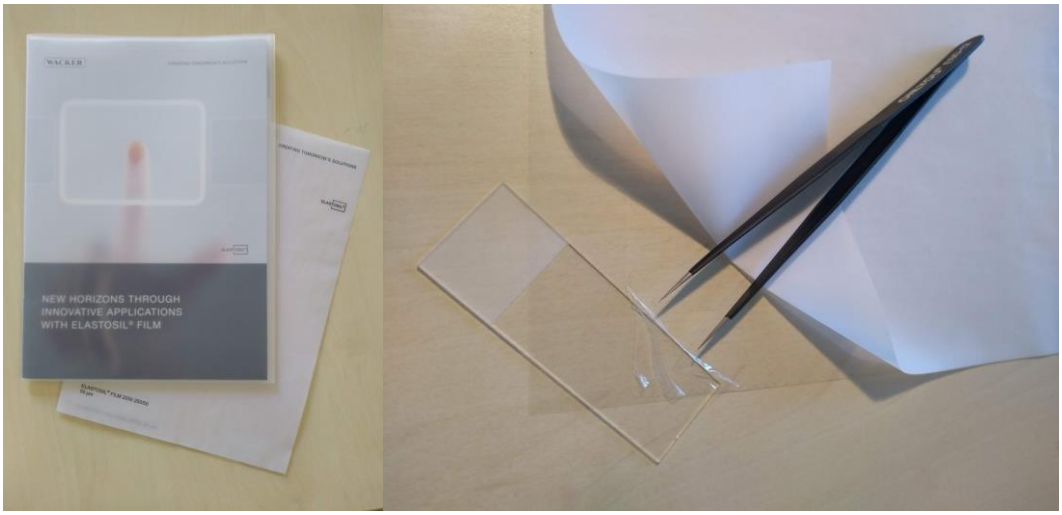

Figure 5.4: left: ELASTOSIL® Ultrathin silicone film - right: 50 µ m thick silicone foil placed on a glass substrate with tweezers

The previously introduced adhesive tape foil fulfils these conditions, expect that some glue contamination remains on the sample. Silicone has an adhesive nature due to Van der Waals forces. A thin film of it fulfils all the above mentions conditions and is applied rather easily. The company Wacker[4] provided testing samples of *ELASTOSIL® Ultrathin silicone film*, with thicknesses of 20, 50, 100 and 200 µm in folders as seen in Figure 5.4. The silicone thin film was delivered on a 100 µm thick PET carrier foils which will be of importance later.

A piece can be cut with a scalpel to fit over a sample. Putting it on top of a sample on a glass substrate, even with tweezers, proofs to be difficult to handle due to its adhesive nature and it sticking to itself. Its adhesive nature, however, minimizes the air inclusion and lets it stick to the glass to hold itself and the sample in place and shield off oil. The

[4] http://www.wacker.com

substrate then needs to be fixated to the table to prevent pulling. Vacuum applicability is not given as the oil would evaporate. The silicone foil, however, failed to adapt adequately to surface abrasions when tested on the Si45-abr sample.

To show no residue is left when this silicone thin film is applied (in contrary to adhesive tape), a piece of film was placed on a polished, clean and flat standard silicone waver. An optical image of the used SI-waver can be seen in Figure 5.5. The image in Figure 5.6 shows the same waver after applying the silicone foil and removing it. Evidently, no significant changes before and after applying a silicone thin film occur, confirming that it does not contaminate samples.

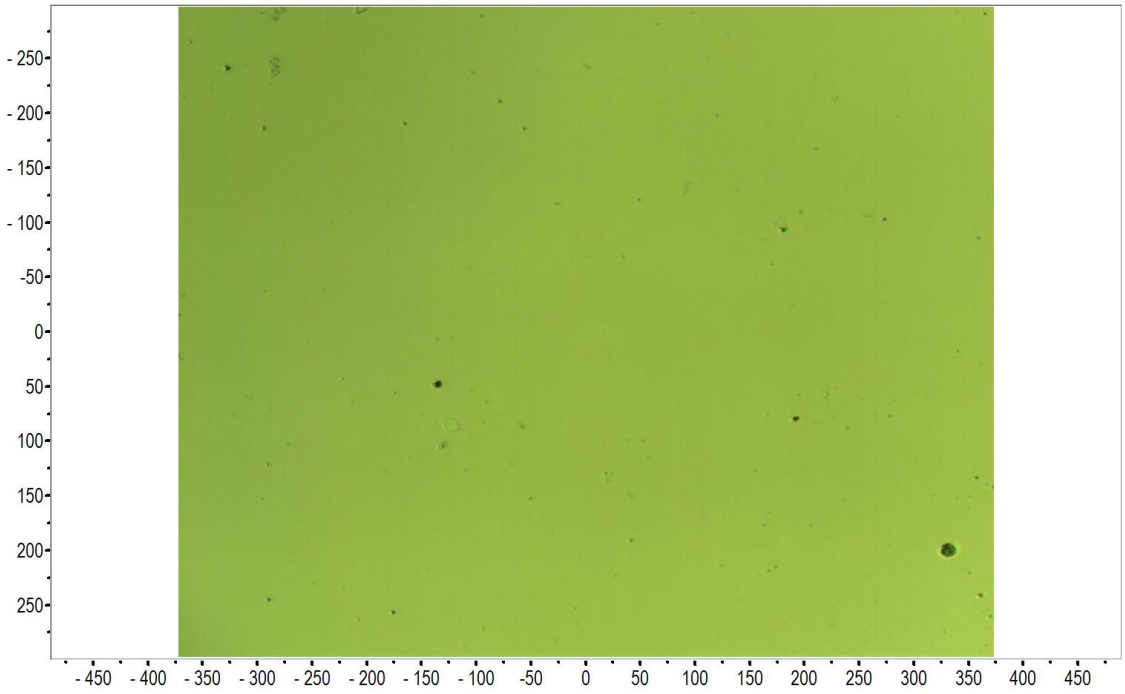

Figure 5.5: Optical image of a Si-waver before applying the silicone thin foil.

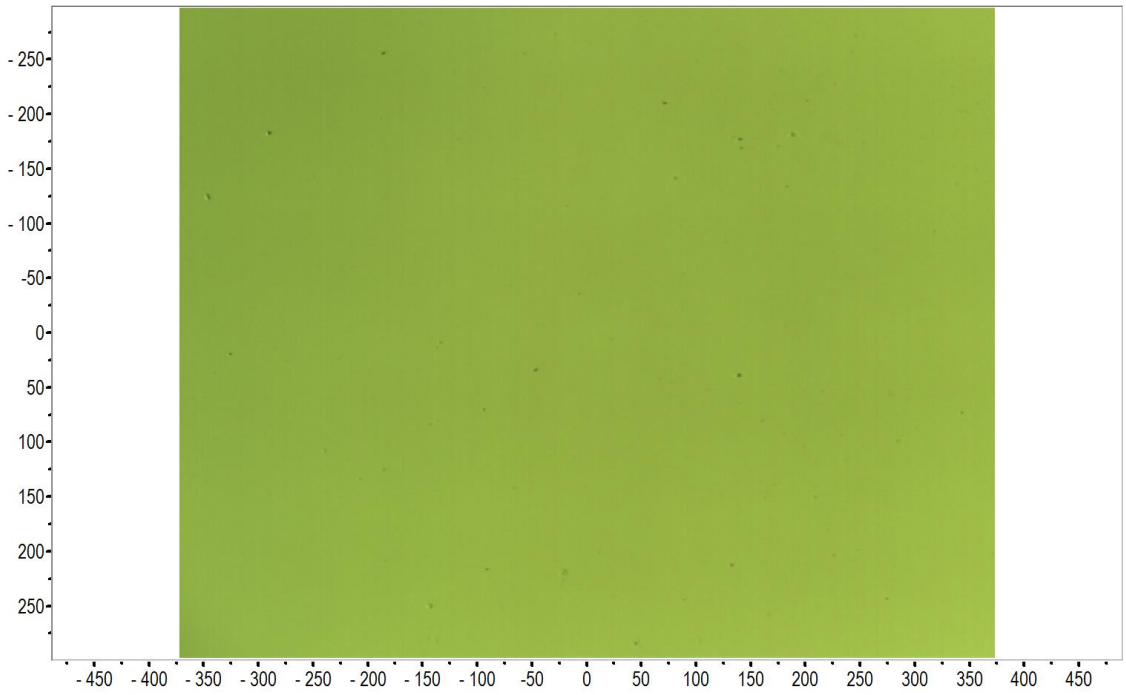

Figure 5.6: Optical image of a Si-waver after applying the silicone thin foil.

A couple of further attempts without any vacuum applications in mind will now be discussed briefly. Unfortunately, none of them have proven to be useful.

5.4 Membrane box

A customary membrane box is readily and cheaply available in nearly every lab. It has two thin membranes in a stable frame that is transparent, can hold samples in place and prevents pull from the oil. The low weight of the box, however, will not prevent the oil from lifting the whole box, wherefore it hast to be taped down. The membrane of the box was not investigated and the detailed specifications including refractive index are unknown.

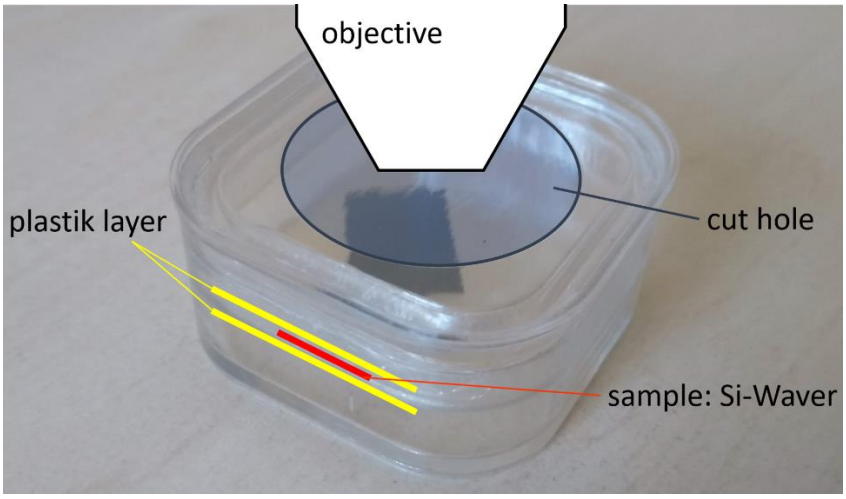

Figure 5.7: Customary membrane box to be cut open to allow direct contact to membrane with immersion objective. A plain silicon waver has been placed between the two membranes.

To make room for the oil immersion objective that must be in close proximity to the sample, the boxes lid was cut open with a rotary grinder. The used box with a piece of silicone waver between the box's layers can be seen in Figure 5.7 where a representation of the objective is visualized. The box, taped on a glass substrate to fixate it and prevent pull from the surface tension of the oil, fits on the table of the Raman microscope and represents a potentially fast, easy and cheap solution. In theory, the optical path is now entirely in media with similar refractive indices: Leaving the objective, into the oil, onward to the upper membrane layer and then into the sample. However, when placed inside a box none of the chosen samples could yield adequate data. It was concluded that either the membrane or the setup is insufficient to serve as a suitable approach. Theoretically, the preparation and handling of the box could have been high but was cumbersome at best. Further research into the membrane box was omitted.

5.5 Wax

Customary wax was thought to seal off the sample from oil, hold it in place on a substrate and adapt to surface abrasions. To prevent pull this substrate must be attached on the table. The used wax melts easily above $T_{melt} \approx 40$ °C and can be dripped onto a sample or a substrate. If the sample withstands the temperatures in this process and will not soak up the wax, this preparation can be undone, and the sample reused. Wax can also be thin-coated to achieve a layer below 200 µm - which is necessary for the used objective to still obtain a signal from the sample. The limiting factor here, the oil immersion objective, could be exchanged with a different immersion objective with larger working distance to elude this problem. First attempts with regular candle wax failed due to its non-transparent solid states. It was thought, that thin enough applied wax through spin coating would let enough light pass to allow measurements. Several attempts have proven otherwise. Few additionally tried waxes showed the same behaviour. Further research into waxes on paraffin or different basis was omitted.

5.6 Gelatine

The same way as wax, regular gelatine used in cuisine can be thin-coated onto a sample. It is mostly transparent (even when dried), removable and does, at first appearance not react with samples. For sample preparation, the instructions on the packages are followed and the obtained solution is spin-coated onto the sample. Overhanging parts can be removed with a scalpel and the glass substrate where the sample rests, fits into the table of the microscope. Measurements were unsuccessful due to not thin enough applied gelatine. In several experiments, the gelatine could not be applied thin enough onto samples to allow measurements with the available objective. This is most likely due to strong forces within the solution resulting in large junks (compared to the wanted thickness) that spread unevenly across a surface it is applied on. An immersion objective with a large enough working distance to penetrate up to several mm of gelatine could potentially yield data, assuming gelatine in this thickness does not absorb or scatter too much light. Additionally, its removal proves to be difficult, which is a knock-out criterion for some samples. Further research on gelatine as a protective layer was omitted.

5.7 Vacuum application

All previously introduced approaches provide no application for usage in extreme low-pressure environment or vacuum, which is needed for the new generation of correlative Raman-SEM microscopes. In this chapter, all approaches that were developed with vacuum applicability in mind are discussed. The basic idea is always to fully enclose the oil droplet to prevent its evaporation.

5.7.1 Oil sphere

To avoid evaporation, the idea was to enclose the drop of oil in a way it is not exposed to vacuum and cannot contact the sample to contaminate it as displayed in Figure 5.8. In the field of “molecular kitchen” in cuisine, edible oils, like olive oil can be processed to form little spheres to imitate caviar. Similarly, it was thought to harden the outer layers of the immersion oil with a chemical process to conceal the still liquid oil in the middle. This would give easy to handle spheres, simply put on top of the sample, giving a removable, refraction free path. The chemical process was thought to alter the oil in a way, that the outer shell would not contaminate the sample with oil, be flexible enough to adapt to the objective and potential surface irregularities and have a similar refractive index as the oil inside the sphere. There are two ways for specification: basic or direct spherification[5] and reverse spherification[6]. For the basic method, a liquid with sodium alginate is submerged in a bath of calcium to form spheres. This method, however, does not work with oil, as the spherification does not stop at any desired time and will harden the whole drop of oil. This itself would not exclude this method for this purpose but the inability of sodium alginate to dissolve in oil does.

[5] http://www.molecularrecipes.com/spherification-class/basic-spherification
[6] http://www.molecularrecipes.com/spherification-class/reverse-spherification/

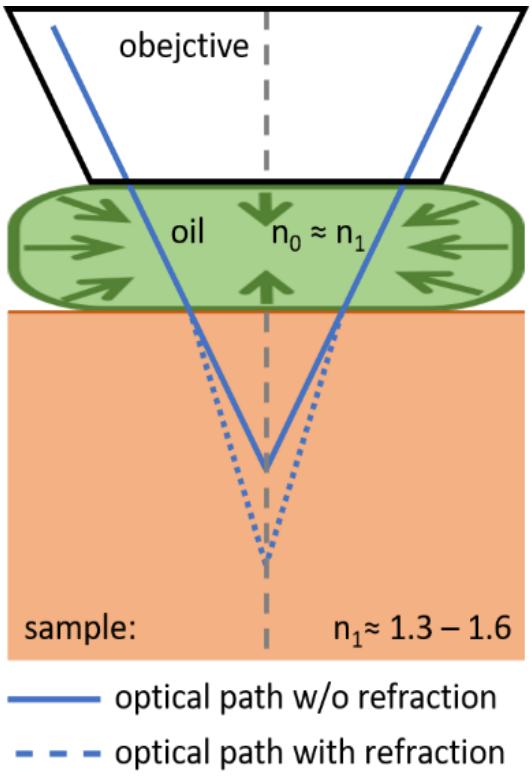

Figure 5.8: Optical path with chemically altered oil-sphere.

The second method, the reverse spherification, potentially can function as a protective, non-refracting layer. Here the sodium alginate is dissolved in water, the bath to drop the oil into. The liquid to be spherified must contain calcium. This method produces spheres that have a hardened shell with a liquid state inside, as only the outer layers of the liquid containing calcium can react with the sodium alginate and solidify.

First attempts with edible oil were successful and produced small spheres. When tried with the necessary immersion oil, only bulky, cumbersome forms were achieved. Several trials could yield none to little better results. None of the produced spheres or more accurately blobs were able to yield reasonable results. After consulting with chemical experts at the Technical University and Karl-Franzens University of Graz it was concluded, that the approach to obtain spheres of immersion oil could potentially work, but would need extensive research and trials. A large problem was stated to arise from the needed properties listed in Table 5.1, especially the refractive index, which must be in the range of common samples ($n_{sample} \approx 1.3 - 1.6$). The chemical approach would include polymer chains with lipophilic and non-lipophilic ends. The creation of a solution with said polymer chains is beyond the limits of this

thesis and outside of the author's field of expertise. Therefore, this approach was ended.

5.7.2 Bubble

The idea of the approach, from now on referred to as "bubble", is to enclose the oil completely, so it cannot contaminate the sample. Additionally, this would prevent evaporation and allow measurements under low-pressure conditions. With this it was thought to create an optical path as seen in Figure 5.9, where the light is constantly propagating in matter with a refractive index in the range of the sample. The grey part in this image represents the device holding two transparent layers that enclose the oil. Between the two layers is a gasket (the black part of the image), which seals the connection between the two layers.

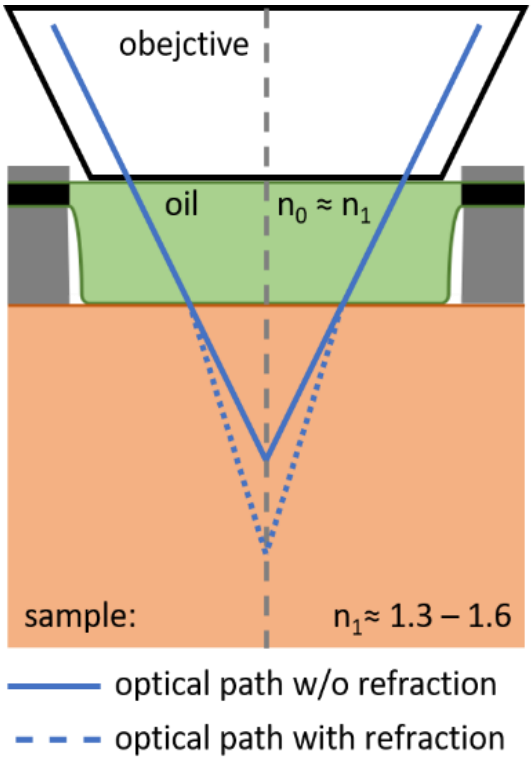

Figure 5.9: Optical path through bubble filled with oil, retainer lateral.

This approach is closely aligned to the one introduced in the 2009 paper *Confocal Raman Microspectroscopy: A Non-Invasive Approach for in-Depth Analyses of Polymer Substrates* [9]. An additional layer was introduced to capsule the oil and prevent evaporation of the oil. A device was built in the workshop of the Institute for Electron Microscopy to hold

two PE foils. It can be seen in the top left image of Figure 5.10. A metal ring with an inner diameter larger than the objective's diameter to fit inside and move in x- and y-direction, with a ring plate attachable on top. In between the base and the plate, two PE foils are placed, with an O-ring between them. The grey part in Figure 5.10 is a gasket which holds the two foils apart and serves as an entry point through which a needle can be injected to fill the space in between with oil. The created bubble can be placed on top of the sample. The pressure inside the bubble is thought to push onto the sample, hence avoids all air inclusions between the bubble and the sample and can adapt to possible surface irregularities of the sample.

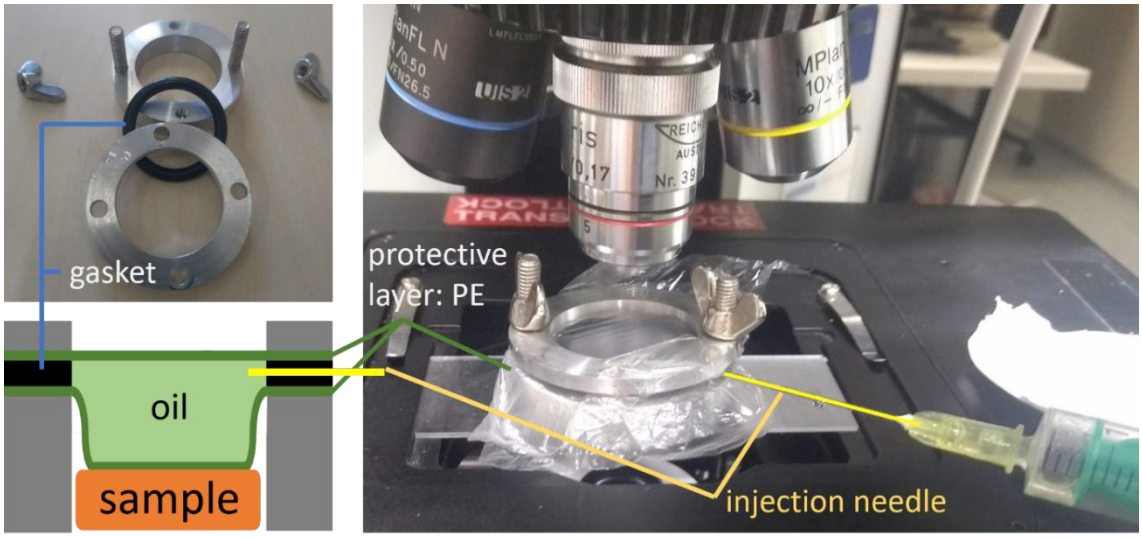

Figure 5.10: Bubble explained

Left top: Dismantled manufactured device to hold two PE-foils as a protective layer and a gasket in between.

Left bottom: Conceptional drawing of the device with a sample underneath.

Right: bubble device in use with an injection needle through gasket to adjust oil level inside the bubble.

The distance between the sample and the objective is rather large with about 2 cm. The used immersion objective with a working distance of < 200 µm is insufficient to conduct measurements with a fully filled bubble. Therefore, the bubble was filled with very little oil, so the distance suffices the objective. This, however, neglects the purpose of the filled bubble, to build pressure on the sample and avoid air inclusions. Attempts to obtain a signal were unsuccessful probably due to air inclusions. The sample was jacked up to minimize the distance from the

specimen through the bubble to the objective, however, even with different settings or filling levels, no conclusive data could be obtained. An objective with a larger working distance or a device with a significantly smaller distance between the objective and the sample might work. As such an objective was not available and the production of this device was rather cumbersome the approach was labelled ”potentially successful”.

5.7.3 Bag

Tomba and Pastor introduced a protective layer between sample and oil, with the sample in a vacuum to suck the layer to the sample [9]. The Bubble approach was intended to enclose the oil entirely and achieve lack of air and an optical path with homogeneous refractive index with the pressure from within the bubble. The idea of the bag approach is to connect the protective layer (PE foil) to the objective. The foil should be stretched, avoiding wrinkles. The oil inside the bag provides a pad that is adaptive to surface irregularities and reduces air inclusions. A representation can be seen in Figure 5.11 where the oil (light green) is held by a protective layer (dark green) which is held by a ring (grey) closely attached to the objective.

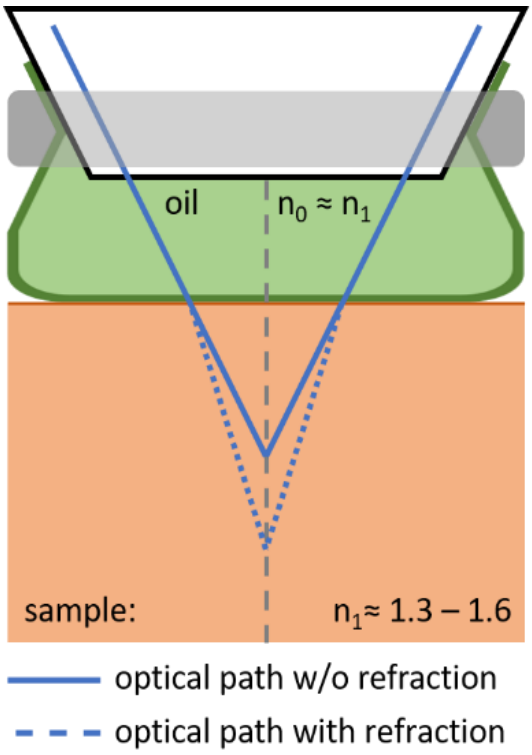

Figure 5.11: Optical path through the bag

The preparation is somewhat cumbersome. The self-made Teflon ring with a small strip inside fits tightly into a notch on the objective. It was manufactured in the institute's workshop and can be seen in the left image of Figure 5.12. With a piece of PE-foil, a bag was formed, and immersion oil put inside. The ring holding the bag was mounted on the objective and the foil stretched tightly to have a small oil bag. Only little adjustments can be made to tighten and stretch the foil before it breaks, so preparation must be done meticulously.

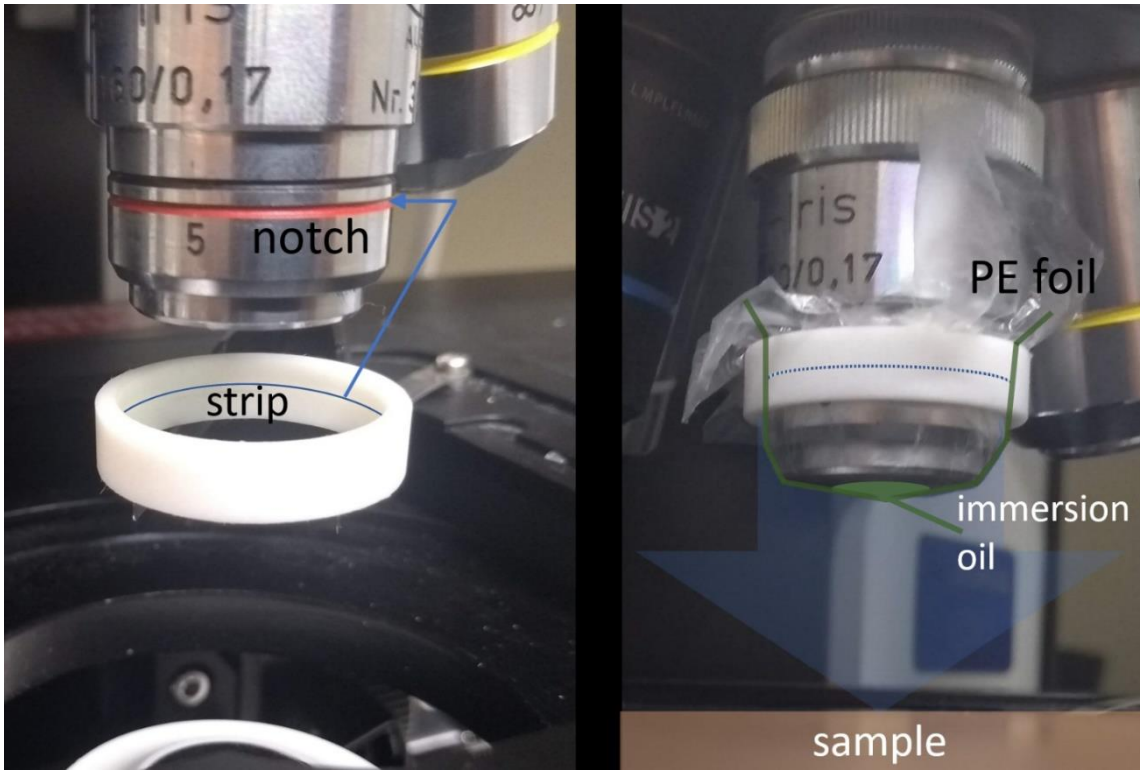

Figure 5.12: Teflon ring for the Bag approach

The Teflon ring in the left image has a strip left when milling that snaps into the notch on the objective. Between ring and objective, a thin layer of PE foil is placed and a drop of immersion oil at the bottom forms a contamination and refraction free approach. The whole setup in the right image is brought into contact with the sample to conduct measurements.

With this setup, displayed in the right image of Figure 5.12, measurements were conducted on a flat Si-wafer, and the results can be seen in Figure 5.13. The red line shows that the signal can be obtained, however, it is widened and still detected in depths of about 30 µm to an amount of about 20% of the maximum detectable signal. Displayed in comparison is the signal obtained directly with oil where the 20% mark

is reached at depth of about 9 µm. This was the reason to halt further research into this approach. The fact that signal can be obtained, howsoever bad in quality, led to the label ”potentially successful” of this approach. It is thought that with a more sophisticated implementation this method could serve as an approach to allow refraction and contamination- free, potentially in a vacuum, measurements in confocal Raman spectroscopy.

Some downward force seems to be necessary to ensure good contact between the foil and the sample. This was originally intended to be achieved by increased oil pressure in the bag. However, regulating the oil pressure accordingly was not possible in this simple design and further issues with the stability of the PE-foil might arise. Consequently, a similar approach including the attempt of a mechanical downward force was tried.

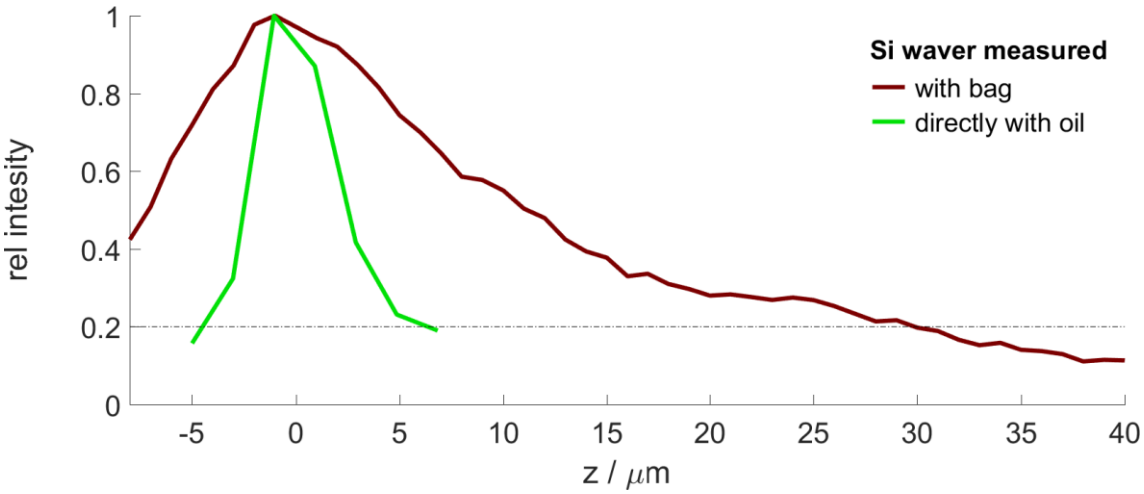

Figure 5.13: Spectrum of flat and polished silicon waver measured with the bag approach in comparison to the same sample measured directly with oil.

Settings: Laser intensity: 100%
Integration time: 0,1 sec per spectrum

5.7.4 Arc

During the trials, it was concluded, that a certain force towards the sample is necessary to have enough connection between the protective layer and the sample for proper measurements. This can be achieved by a material that, in addition to all the necessary conditions from Table 5.1, is rigid enough to provide said pressure. It is mounted to a self-made device (grey part in Figure 5.14) that fits on the objective and can hold a strip of transparent foil, so it forms a downwards facing arc. The open sides (z-axis (out of the picture) in Figure 5.14) are problematic for vacuum applications as any oil inside would evaporate. However, if the tests in atmospheric pressure turn out to be successful, closing the sides and protecting the oil from vacuum should be manageable. To achieve surface adaptability, additional soft outer layers could be introduced.

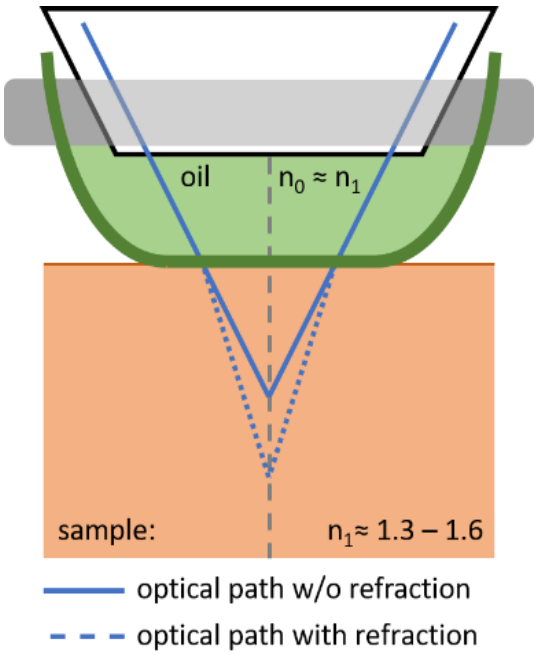

Figure 5.14: Optical path through oil held by an arc mounted with a frame to the objective.

The quest remains which materials would be suitable for the outer shell of the arc. To achieve vacuum applicability, surface adaptability *and* the necessary downward force a stiff silicone film would be suitable, but plain, stiff silicone below a thickness of 100 µm could not be found. However, examining the earlier mentioned carrier foil (5.3) on which the silicone foil was delivered, the combination of the stiff PET and the thin,

adaptive silicone foil was thought to do just that. The delivered PET foil has a thickness of 100 µm. With the working distance of the oil immersion objective of 200 µm, 100 µm remain available.

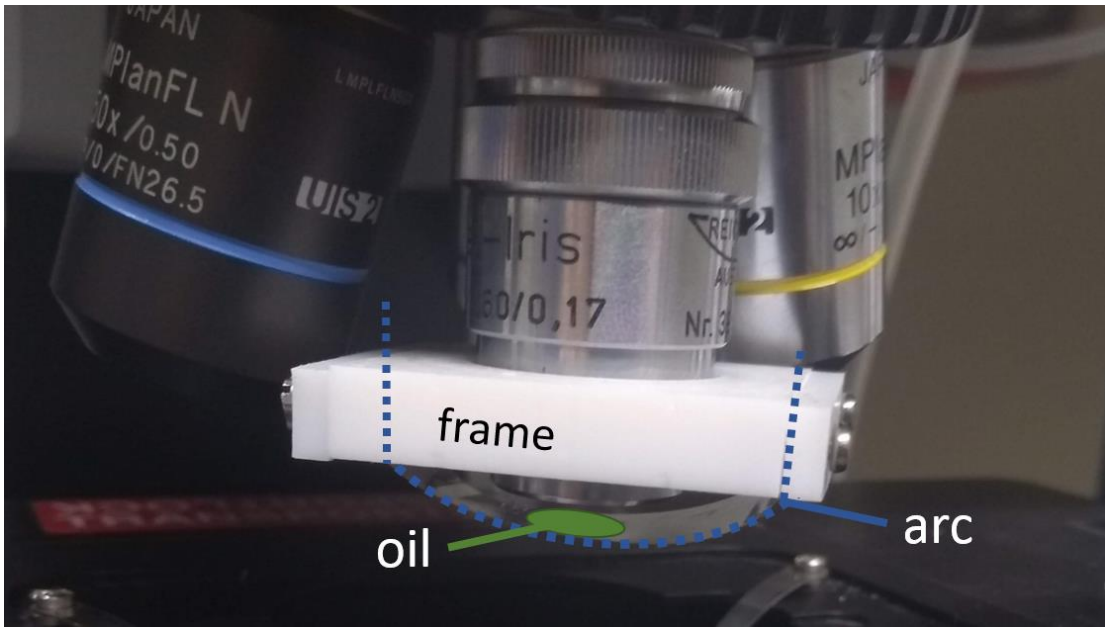

Figure 5.15: Frame for the arc approach

The frame holding the arc is mounted on the objective with a drop of immersion oil between the arc and objective. The image shows the loosely fixated arc. Measurements are conducted with the arc as tight to the objective as possible to have as little working distance occupied as possible.

The first version of the arc approach was done by cutting the silicone thin film, together with the foil it was delivered on, which was thought is plain PET. This strip was then placed into the holding device seen in Figure 5.15. Several measurements failed and no meaningful data was obtained.

The two components are known to not alter the laser. PET from literature and silicone from 5.3. So, the combination should work just fine. As the silicone foil was tested already, it was concluded, that the carrier foil must alter refraction and prevent successful measurements. The next logical step was to test the PET of the carrier foil on its own.

PET on its own does not have an adaptive surface for applications on samples with abrasive surfaces, however, it does provide the stiffness to achieve the necessary downward pressure when mounted in the arc device. The PET carrier foil without the silicone thin film, however, did

not yield any meaningful data, either. It was theorized that the curvature of the arc could interfere with the Laser beam.

To test the general capability of functioning as a protective layer, the PET carrier foil was tested on its own – without the mounting device. Due to the thickness, this film cannot be wrapped like the PE foil, hence it is cut in the desired size and must be fixated with adhesive tape outside the optical path to hold the sample in place and shield it from oil like displayed in Figure 5.16. None of the examined samples yielded conclusive data with PET as a protective layer. Several variations in how the foil was fixated were tested, however, this setup was unable to yield any usable data. This is in contradiction to literature knowledge of PET as it should be permeable to the light of the frequency of the laser.

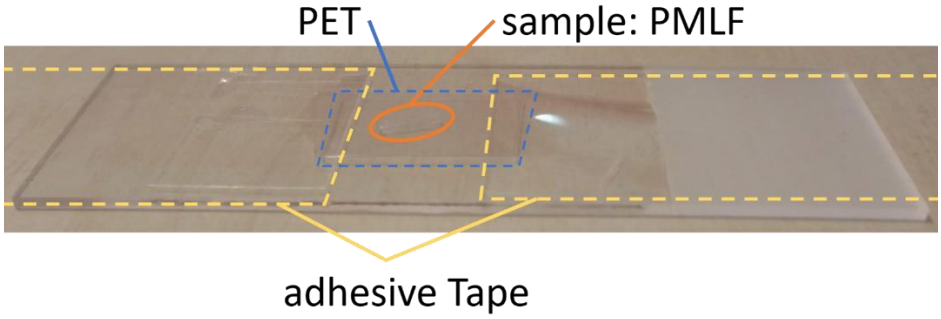

Figure 5.16: Sample protected with 100 µm PET, fixated with adhesive tape on an object slide.

Based on these findings, it was tested, if the foil alters the optical path. Therefore, the laser focus was tested. When focused on a clean and flat silicon waver, the laser, when adjusted correctly, should be focused in a small circular spot like it can be seen in Figure 5.17 (a). To yield usable data, the laser must be focused like this. However, when the PET thin layer was placed in the optical path, the focus could not be adjusted, and the best settings resulted in a diverged spot as seen in Figure 5.17 (b), which cannot produce any quality data.

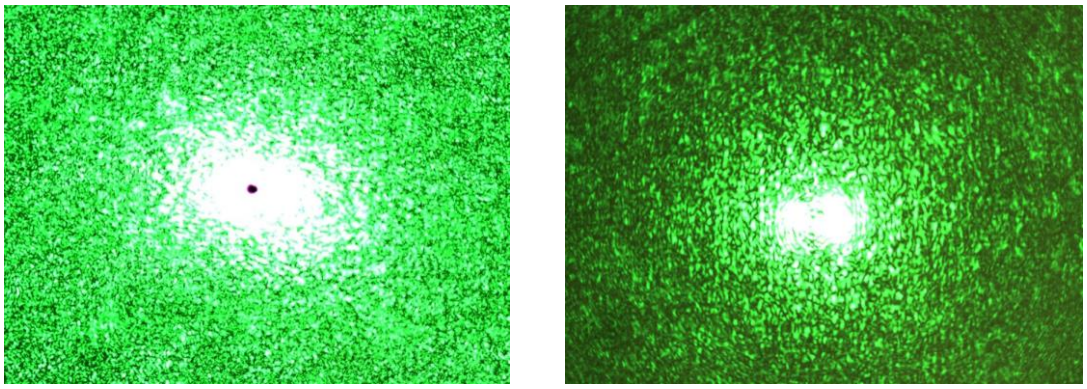

(a) The green laser (ω = 532.16nm) focused on a clean silicon waver.

(b) The green laser (ω = 532.16nm) focused on a clean silicon waver through a PET foil of 100 µ m thickness.

Figure 5.17: Comparison of the laser focus, when focused on silicon waver through air to when focused through air and a 100 µm thick PET layer.

After more thoroughly examining the obtained spectra of the PET foil, it was found that the composition must have additional ingredients, probably for the intended purpose of serving as carrier foil for silicone that allow an easier separation of the foil from the carrier PET. The exact ingredients and recipe of the production of their PET-like material are kept secret by the producing company. When pure PET was examined the expected behaviour occurred. It was thus concluded that a new approach using a self-made layer system might be useful.

A PET foil of 100 µm thickness served as carrier foil on top of which liquefied polymers were deposited and spread with a doctor blade method to create a defined thickness of 50 µm. Four different layer systems were created to test different adaptive layer materials. Many thanks go to the Institute of Analytical Chemistry and Food Chemistry of the Technical University of Graz, under the supervision of Borisov, Sergey, Assoc.Prof. kand. They were kind enough to manufacture these four different layer systems with the doctor blade method, each on top of a 100 µm thick PET carrier foil:

Si33	-	Silicon 33% in Cyclohexan
HyTh	-	6% HydroThane 5-93A in Chloroform
Sty-THF	-	15% Styrene-Butadiene ABA Block in Tetrahydrofuran
Sty-Ch	-	15% Styrene-Butadiene ABA Block in Chloroform

These four multi-layer systems were tested the same way as PET. Flat on a sample, not mounted on the arc holding device. The layer consisting of Styrene- Butadiene was unable to yield any data. This was true for both preparation methods: dissolved in Tetrahydrofuran and in Chloroform. The layer consisting of HyTh, also was unable to produce meaningful data. It was theorized that both, Styrene-Butadiene and Hydrothane alter the laser beam and disallow for quality data, however, no tests were conducted to determine the exact behaviour of the material.

The layer system consisting of silicone applied on PET as a carrier foil was the only composition tested that yielded quality data. The results are discussed in 6.3.

6 Results and discussion

Following the last chapter, where the oil-contamination free approaches were introduced the results obtained on the test samples from chapter 4 are shown and discussed in this chapter in the same order as they were introduced.

Comprehensive results on several main samples were achieved by the adhesive tape and silicone foil approaches. Additionally, results on the Si45 wafer were achieved by the arc approach which is also discussed in this chapter.

A summary of how well these approaches worked can be seen in the following Table 6.1.

Table 6.1: Compression overview of oil-contamination free approaches

Compression	sample			
approach	Si45	PMLF	PSuB	Si45-abr
adhesive tape	≈ 5,5 %	≈ 4,0 %	not computable	≈ 5,7 %
silicone foil	≈ 9,5 %	≈ - 8,0 %	not conducted	not computable
arc - PET + silicone	≈ - 8,0 %	not conducted	not conducted	not conducted

6.1 Adhesive tape

Adhesive tape is applied on a sample, either on a glass substrate or on a sample embedded in resin, on top of which a drop of immersion oil prevents refraction with the oil immersion objective immersed in the oil. All setups must be fixated to the microscope's table to prevent pull from the oil's surface tension.

6.1.1 Si45 with adhesive tape

The obtained signal of the Si45 sample measured with adhesive tape as contamination protection can be seen in Figure 6.1 where it is compared to the results measured directly with oil. The tape and glue can clearly be distinguished in the 2D scan in the top right image, as well as in the graph on the bottom of the figure where the spectra over depth are displayed (dashed line). Also drawn is the spectrum of the Si45 obtained through measurement directly with oil (solid line). Both methods display a similar loss of intensity over depth. The top left image of the figure shows the 2D scan of the Si45 measured directly with oil - it is in scale to its neighbour. The compression was calculated through the depth angle, relative to the compression of the Si45 measured directly with oil and is about 5% which is within tolerable range and can be considered negligible in many applications. The information loss was calculated by a linear fit through the 45° part of the SI-waver as seen in the bottom part of Figure 6.1. The calculations show an almost constant count over more than 70 µm with and without tape as a protection method. This means that adhesive tape is – at least for an ideal sample –capable of protecting samples from oil. The contamination of the sample with glue, however, remains.

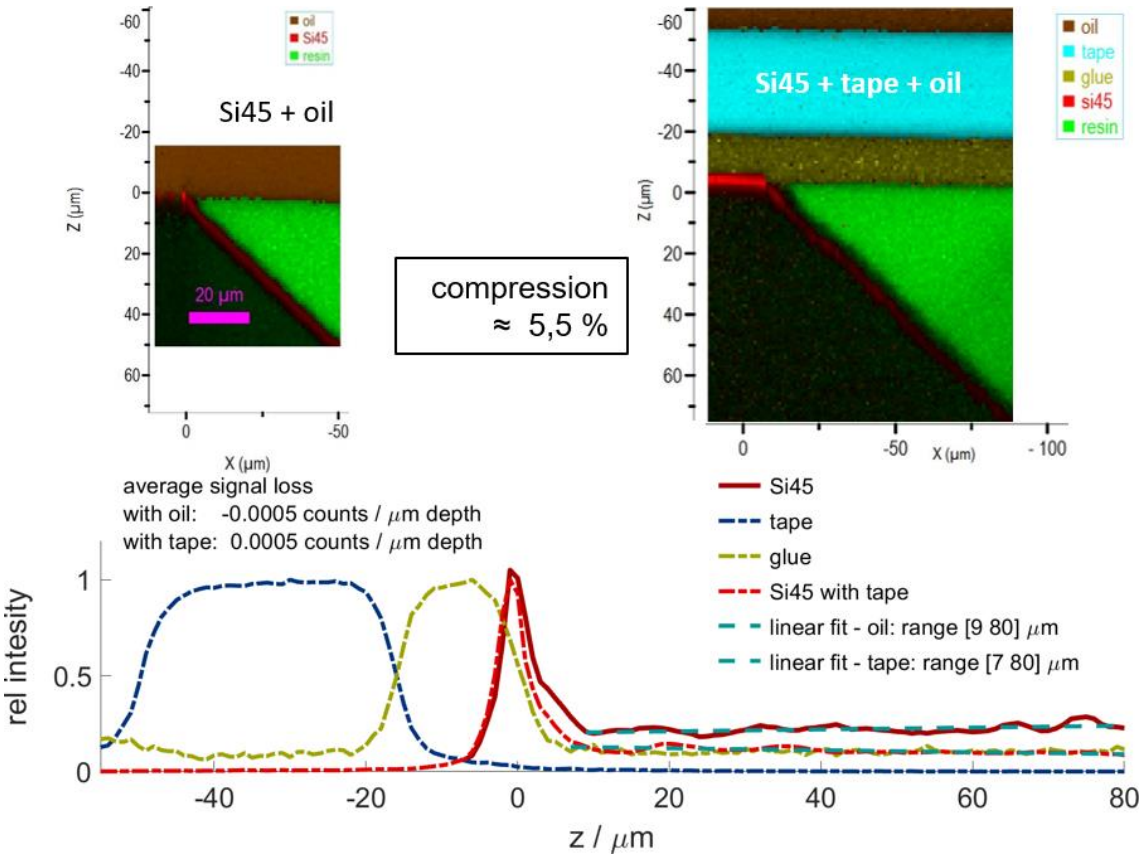

Figure 6.1: Comparison of Si45 with(out) tape and oil

The top two images show the 2D-scan of the Si45 sample measured directly with oil (left) and with adhesive tape and oil (right) as contamination prevention.

The image at the bottom shows the intensity of each material's signal over depth, measured with oil (dashed line) and with adhesive tape and oil (solid line).

Settings: Laser intensity: 100%
Integration time: 0,1 sec per spectrum

6.1.2 PMLF with adhesive tape

The PMLF sample protected with adhesive tape yielded data displayed in Figure 6.2. The 2D scan obtained with adhesive tape is in the top right image with the reference - PMLF directly with oil - left to it. Seen in the bottom is the intensity over depth of both measurement methods where the different layers are clearly distinguishable. The thickness of each layer matches the values determined on the cross-section.

The graphs of both measurement methods of PMLF show hardly any difference in loss of intensity which is in line with the results in the previous chapter. The calculated compression is within tolerable limits with 4% compression relative to the measurement done directly with oil. Adhesive tape, therefore, is capable of protecting not only ideal samples, as shown in the previous chapter, but also samples consisting of layers.

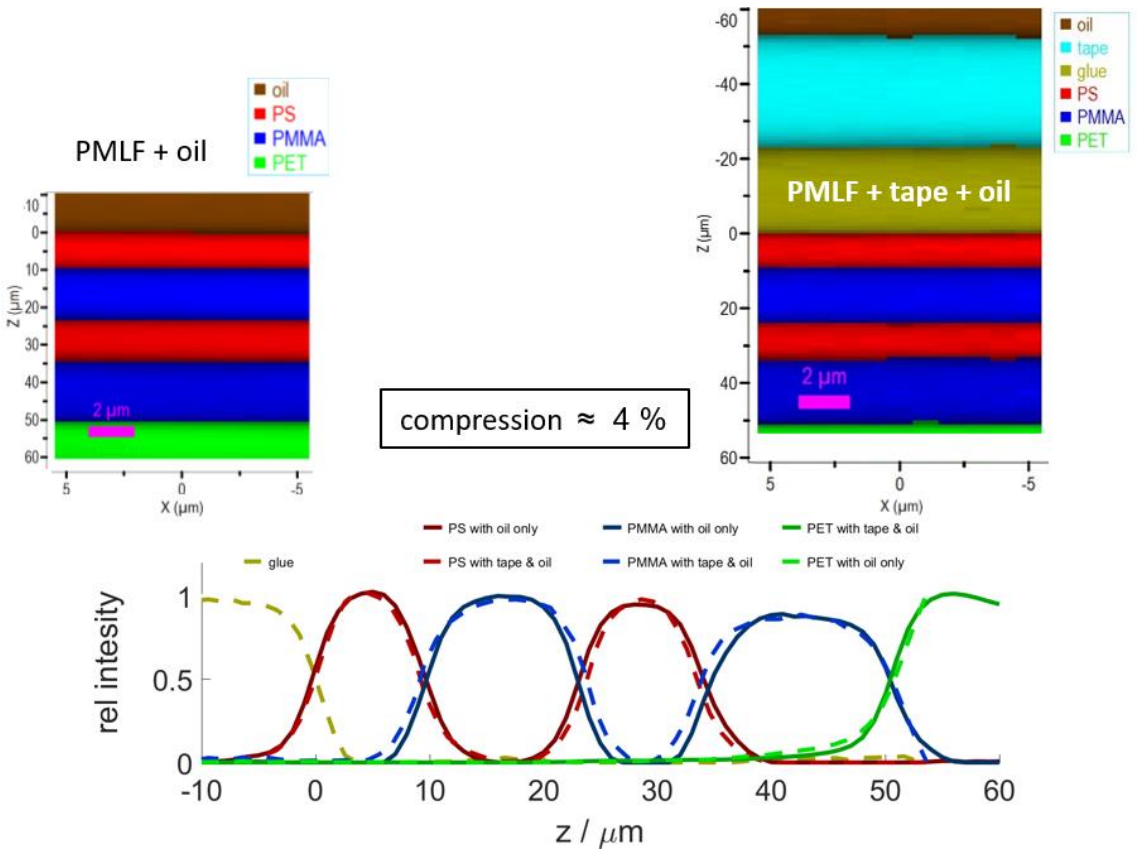

Figure 6.2: Comparison of PMLF with(out) tape and oil

The top two images show the 2D-scan of the PMLF sample measured directly with oil (left) and with adhesive tape and oil (right) as contamination prevention.

The image at the bottom shows the intensity of each material's signal over depth, measured with oil (dashed line) and with adhesive tape and oil (solid line).

Settings: Laser intensity: 100%
Integration time: 0,21 sec per spectrum

6.1.3 PSuB with adhesive tape

The Raman Signal of the PSuB can be seen in figure 3.3.3. 15 µm thick slices of embedded beads were protected by adhesive tape and were investigated to generate a 3D-map. The results can be seen in Figure 6.3 where the left image shows all areas present in the prepared sample. The oil in the top is coloured brown, tape below is blue with its glue in green below. It was concluded that the small yellow fragment between the oil and tape layer is unknown residue which was not investigated further. Beneath the protective layers of the adhesive tape lies the resin (yellow), embedded in which are the PSuB. Zooming in to the PSuB, digitally removing all other layers and interpolating the edges of the beads results in the right image of Figure 6.3. One can distinguish the different beads and estimate their rough sizes to be below 10 µm. With this sample, however, the calculation of a compression relative to the measurements with oil only are impossible, therefore disallowing statements of information loss and compression. As the previous two chapters have shown, that adhesive tape does not alter with the measurement and the rough shape and sizes of the beads could be distinguished these results confirm that adhesive tape can be used for three-dimensional samples as well.

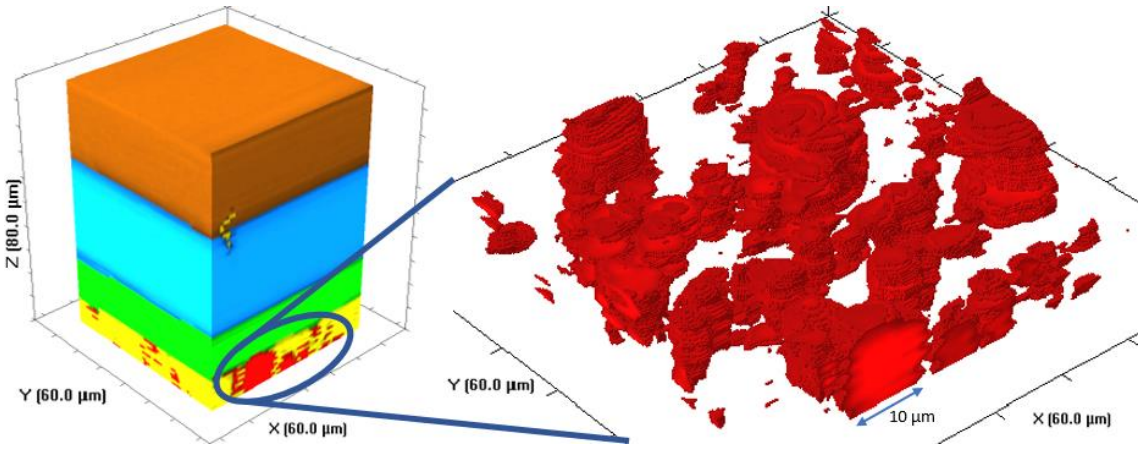

Figure 6.3: PSuB with adhesive tape – 3D model

The left image shows a 3D map of the PSuB, embedded and cut into 15 µm slices, protected by adhesive tape and measured with oil. The red parts are the beads, resin is yellow, glue is green, tape is blue and oil is brown. Also seen is an unknown fragment, not investigated further - the yellow part reaching from the tape into the oil.

The right image shows only the enhanced, interpolated PSuB.

Settings:	*Laser intensity:*	*50%*
	Integration time:	*1,2 sec*

6.1.4 SI45-abr with adhesive tape

The obtained signal of the Si45-abr sample measured with adhesive tape as contamination protection can be seen in Figure 6.4 where it is compared to the results measured directly with oil. The tape and glue can clearly be distinguished in the 2D scan in the top right image, as well as in the graph on the bottom of the figure where the spectra over depth are displayed (dashed line). Both methods display a similar loss of intensity over depth. The top left image of the figure shows the 2D scan of the Si45 measured directly with oil – even though the axis is halved they are in scale to the top right image as the ratio of the z and x-axis is constant. The compression was calculated through the depth angle, relative to the compression of the Si45 measured directly with oil and is about 5.7% which is within tolerable range and can be considered negligible in many applications. It also is similar to the compression found in the Si45 sample in chapter 6.1.1. Information loss could not be calculated due to the blurring. The surface abrasions of the sample cannot be distinguished; however, the purpose of this measurement was to show that adhesive tape will neglect any gas inclusions which would lead to refraction. This could be confirmed.

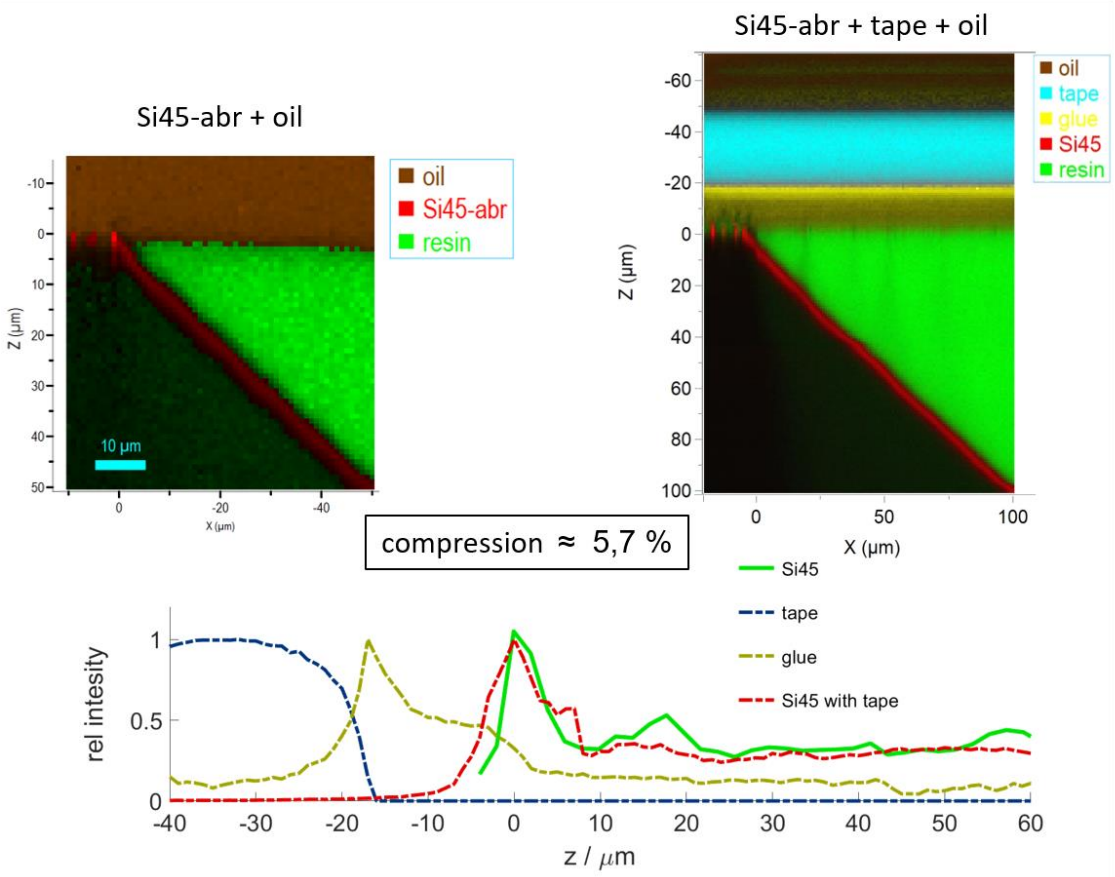

Figure 6.4: Comparison of Si45-abr with(out) tape and oil

The top two images show the 2D-scan of the SI45-abr sample measured directly with oil (left) and with adhesive tape and oil (right) as contamination prevention.

The image at the bottom shows the intensity of each material's signal over depth, measured with oil (dashed line) and with adhesive tape and oil (solid line).

Settings:	*Laser intensity:*	*50%*
	Integration time:	*1,2 sec*

6.2 Silicone thin film

The silicone thin film was delivered on a carrier foil which was introduced in chapter 5.3. It can be cut and placed on top of the sample to be examined, either directly on the embedded specimen or laying on a glass slide. Listed in the subsequent chapters are the results of the scans conducted with this silicone thin film as a protective layer on the used samples.

6.2.1 Si45 with silicone thin film

The silicone thin film was used to protect the Si45 sample. The results can be seen in Figure 6.5, where, again, the top left image is the reference measurement of Si45 measured directly with oil. The top right image represents the sample protected with the silicone thin layer and in the bottom image the signal over depth of both variations is displayed.

The intensity loss of the reference measurement in the bottom image (solid line) is almost identical to the measurement including the silicone thin layer (dashed line) and is constant and about zero for more than 70 µm. The calculated compression, relative to the measurement done directly with oil is about 10%.

This shows that the silicone thin film, like adhesive tape, is capable of protecting an ideal samples and this without the disadvantage of glue.

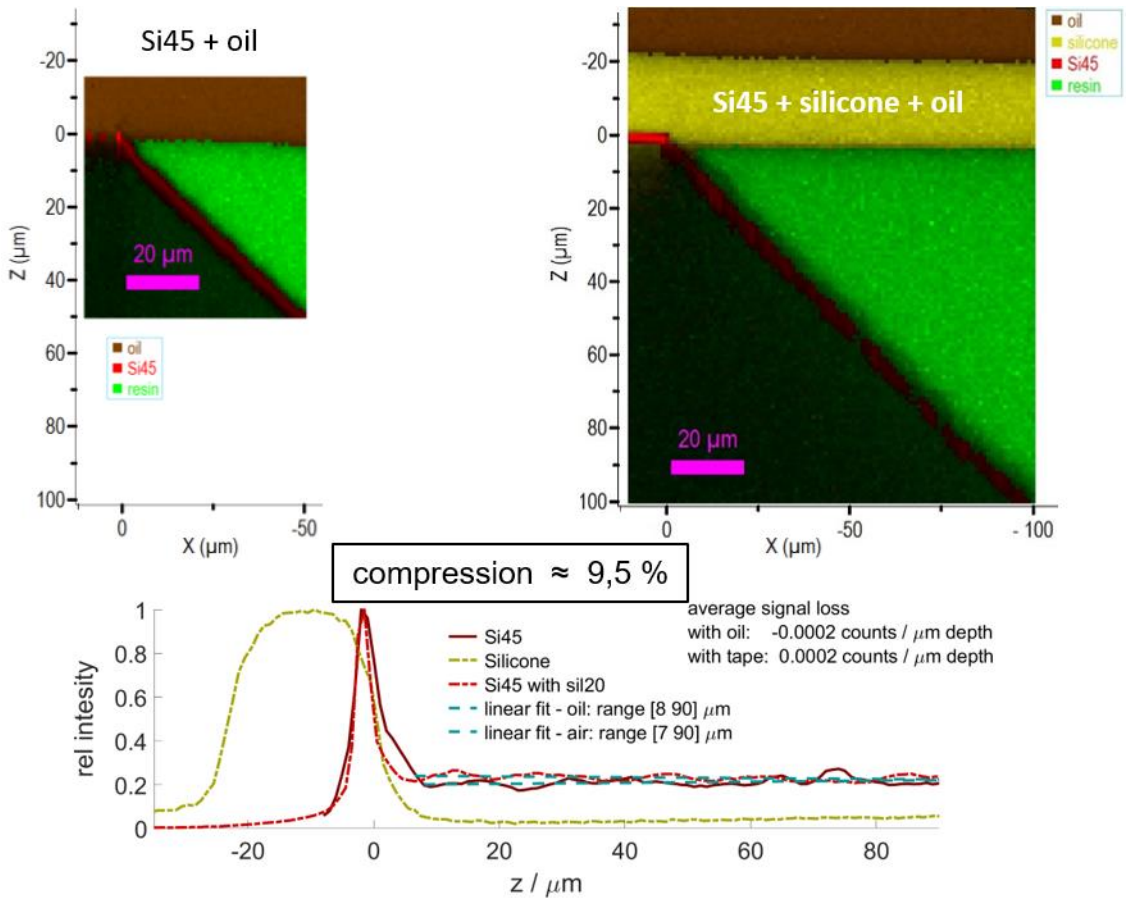

Figure 6.5: Comparison of Si45 with(out) silicone and oil

The top two images show the 2D-scan of the Si45 sample measured directly with oil (left) and with the silicone thin layer and oil (right) as contamination prevention.

The image at the bottom shows the intensity of each material's signal over depth, measured with oil (dashed line) and with the silicone thin layer and oil (solid line).

Settings: Laser intensity: 100%
Integration time: 0.05 sec

6.2.2 PMLF with silicone thin film

The results of the measurement, where the PMLF sample was protected by a silicone thin layer can be seen in Figure 6.6, where, again, the top left image is the reference measurement of Si45 measured directly with oil. The top right image is the sample protected with the silicone thin layer and in the bottom image, the signal over depth of both variations is displayed.

The intensity loss of the reference measurement in the bottom image (solid line) is within the expected range. The loss of intensity in the measurement including the silicone thin layer as protection is evident and significantly larger than the loss of intensity in the reference. In addition to fewer counts of photons, a different depth origin can be observed. Unexpectedly, the signal was not compressed but stretched. This can be seen in the 2D scan, where the PET layer starts in a depth of about 55 µm instead of the expected 50 µm like in the reference, as well as in the bottom graph. Here the layers measured with silicone seem to have a greater thickness than when measured directly with oil. The measurement conducted with a silicone thin foil as protective layer seems to stretch the optical path by 8%, however, it is possible that the sample does not have consistent thickness which was not investigated.

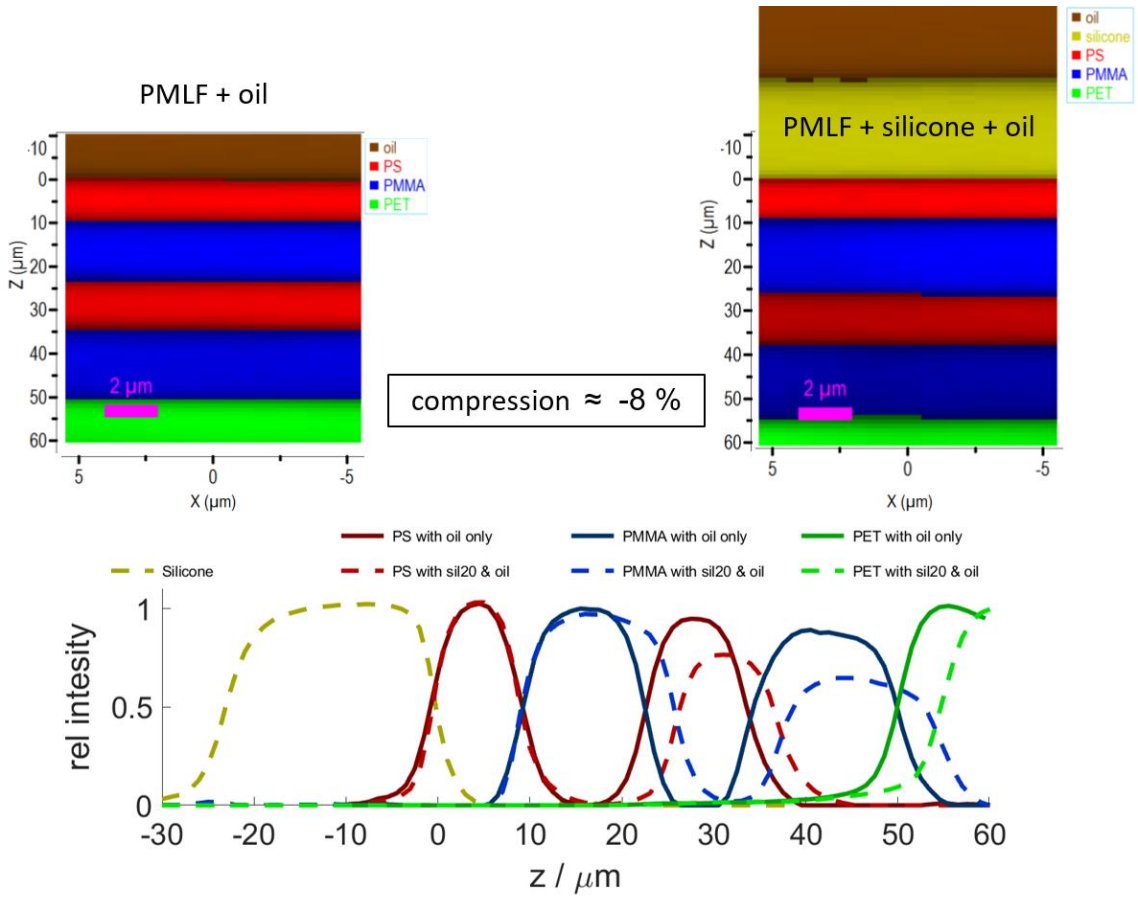

Figure 6.6: Comparison of PMLF with(out) silicone and oil

The top two images show the 2D-scan of the PMLF sample measured directly with oil (left) and with a silicone thin layer and oil (right) as contamination prevention.

The image at the bottom shows the intensity of each material's signal over depth, measured with oil (solid line) and with a silicone thin layer and oil (dashed line).

Settings:	*Laser intensity:*	*100%*
	Integration time:	*0.9 sec*

6.2.3 PSuB with silicone thin film

As noted in Table 6.1, the test for the sample PSuB with the silicone thin film as a protective layer was not conducted. This is since the volume necessary to display the sample with an ample volume, as well as the protective layer and some of the oil is rather large. The scanned volume for this sample protected with adhesive tape (chapter 6.1.3) was 60 x 60 x 80 µm. With the necessary integration time of 1.2 seconds and 2 accumulations for noise reduction, the measurement time results in 8 days of constant measurement (not accounting for movement-time of

the stage nor preparation). The microscope was not available to be occupied for another measurement of this length. The purpose of the sample PSuB was to have a realistic, three-dimensional representation of samples and if protective layers would allow for measurements of such. The measurement conducted with adhesive tape as protective layers was able to confirm that.

6.2.4 SI45-abr with silicone thin film

The results of the measurement, where the Si45-abr sample was protected by a silicone thin layer can be seen in figure 6.2.4, where the top left image is the reference measurement of Si45-abr measured directly with oil. The top right image is the sample protected with the silicone thin layer and in the bottom image, the signal over depth of both variations is displayed.

The bottom image shows, that the embedded silicon yields a similar relative intensity to the measurement directly with oil up to a depth of about 15-20 µm. However, the 2D map shows a different image, with a poor quality and wrongly identified contributions, probably due to a bad contact and complex refraction/reflection on the rough sample surface. The silicone thin film appears to be unable to adapt adequately to surface roughness.

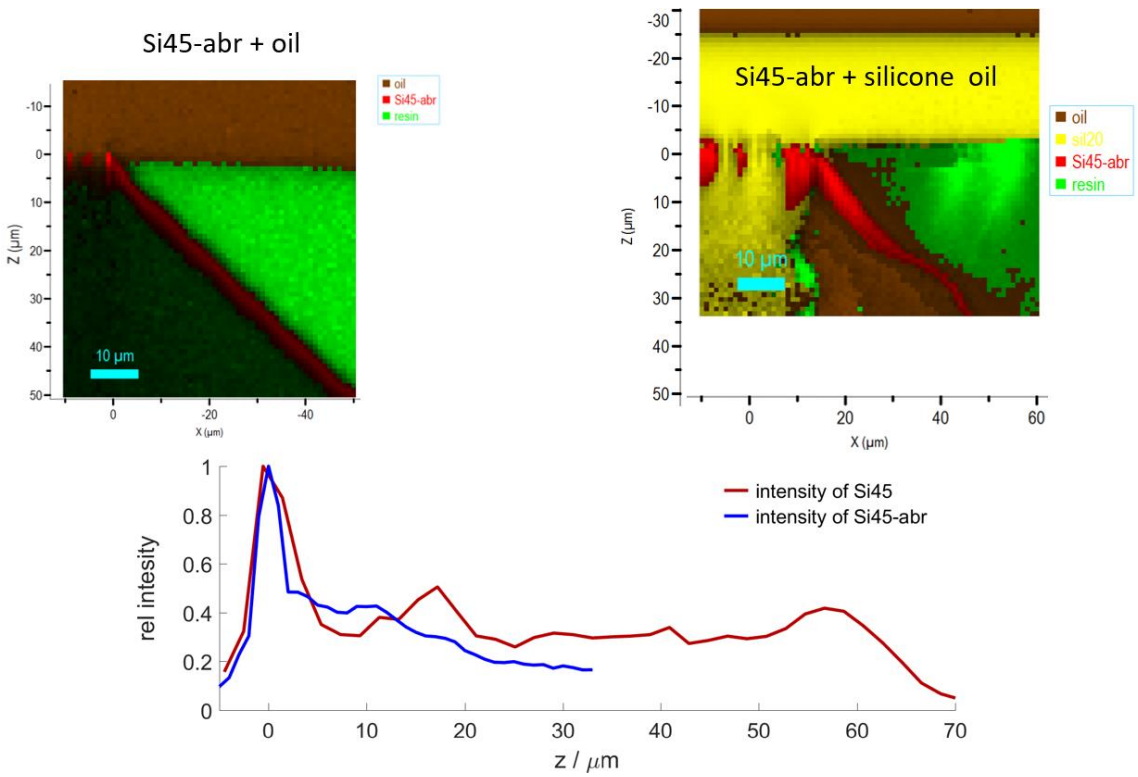

Figure 6.7: Comparison of SI45-abr with(out) silicone and oil

The top two images show the 2D-scan of the Si45-abr sample measured directly with oil (left) and with the silicone thin layer and oil (right) as contamination prevention. The image at the bottom shows the intensity of each material's signal over depth, measured with oil (red line) and with the silicone thin layer and oil (blue line).

Settings: Laser intensity: 100%
Integration time: 1.25 sec

6.3 Arc

The initially tested arc, consisting of the silicone thin film on its delivering foil PET, yielded no quality data. From the 4 manufactured compositions (PET as carrier foil, different adaptive materials towards the sample) the only composition yielding quality data was the setup with 33% Silicon applied in a solution of Cyclohexan.

The resulting 2D map can be seen in Figure 6.8 where in the top right image all layers are distinguishable. This measurement was performed with the layer flat on the sample and not mounted in the arc holding device. It is in comparison to the measurement of Si45 done directly with oil (same scale) and the compression is about 8%, calculated through the depth angle. The bottom image in the same figure shows

the mean intensity over depth of both maps the reference is a dashed line and the layers of the setup with PET and silicone are solid lines.

The intensity over depth shows a larger signal of silicon when measured with the layer system then the reference. However, the 2D map shows that the signal is detected over a large depth which means the layers disperse the detected signal which would usually be a disqualifier. However, the purpose of this approach was to show if PET with an additional layer could be used to protect a sample, which can be confirmed. Unfortunately, for practical purposes, the PET-silicone layer system remains insufficient. Measurements with the silicone thin film on PET in the arc did not yield any data, probably due to additional refraction effects arising due to anisotropy in the bending foil, which compounds with the already limited performance of the foil on its own.

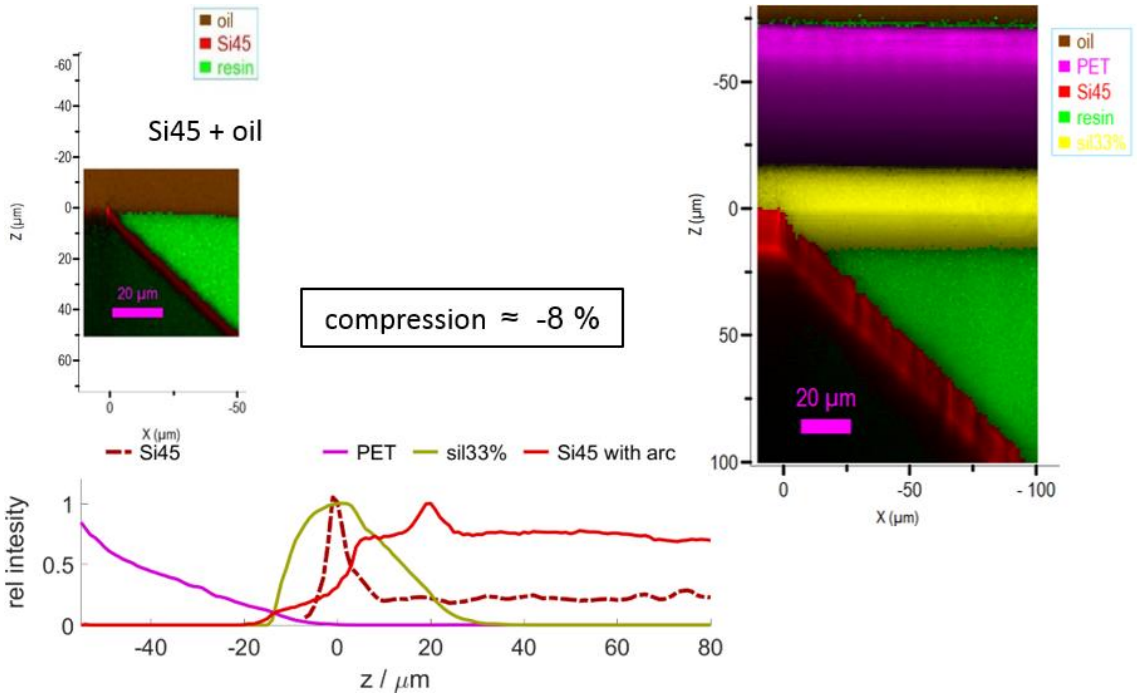

Figure 6.8: Comparison of Si45 with(out) flat sil33 and PET and oil.

The top two images show the 2D-scan of the Si45 sample measured directly with oil (left) and with the arc material consisting of silicone and PET (right) as contamination prevention not in the arc device but flat on the glass slide.

The image at the bottom shows the intensity of each material's signal over depth, measured directly with oil (dashed line) and with the flat arc and oil (solid line).

Settings:	*Laser intensity:*	*50%*
	Integration time:	*1,6 sec per spectrum*

7 Outlook

Considering the results of the arc approach, a measurement technique could be developed, that allows for refraction and contamination-free, 3D, confocal Raman microscopy conducted in a vacuum and possibly automatically.

For this goal, further research would be needed to solve the refraction/defocusing issue arising from the many layers of the arc. The stiff layer in the arc approach provides the necessary pressure towards the sample, and the second layer adapts to the sample to neglect air inclusions. If, for example, a polymer could be found, that can provide said pressure, is adaptable to the surface, has a refractive index of the sample to be investigated and is thin enough to allow the used objective to gather photons from the area to be examined, automatable measurements could be possible.

If this setup could be enclosed to the objective and hence shield the oil from the vacuum, this setup could also be used in correlative Raman-SEM microscopy.

8 Conclusion

The refraction in three-dimensional, confocal Raman spectroscopy due to phase transition is known in scientific circles. The resulting compression and increasing loss of information over depth were shown in this study. The most demonstrative case is a silicon waver embedded at 45° (Si45). The silicon yields a strong Raman signal and the angle of embedding gives immediate information on compression due to the change of angle. The resulting compression was calculated to be about 47% and the average loss of signal was 3.9 times higher when measured with air, instead of oil (Figure 4.1) as compression prevention.

Several different approaches were tried with only two of them proving to be potentially usable (overview in Table 6.1): the adhesive tape and a silicone thin film of 20 µm thickness. When applied on samples the adhesive tape showed compression of 5.5% and 4% on the Si45 and PMLF sample respectively. The loss of intensity over depth were similar compared to the results obtained directly with oil. The adhesive tape is the most practical approach found. It is easy to apply, reliable and readily available. However, the contamination of the surface with glue remains an issue.

The second protective layer - the silicone thin film - showed similar behaviour. Compression of the measurement of the Si45 was about 9.5%. The compression of the second sample was negative, meaning stretching of about 8 % occurred.

The adhesive silicone thin film eliminates the glue contamination issue of the adhesive tape at the cost of being somewhat more difficult to handle, less reliable on rough surfaces and of course less available then regular adhesive tape.

Both refraction prevention methods (adhesive tape and silicone) need little preparation but are not applicable under low pressured conditions, such as in a chamber of an electron microscope where recently, more frequently Raman microscopes are included.

Given the recent development of correlative Raman-SEM microscopes, approaches were tried to allow 3D, confocal, refraction free, immersion microscopy even in a vacuum. The general idea is to enclose the necessary oil to the objective. This was done by a device holding a stiff layer that encloses the oil and provides necessary pressure towards the sample - the arc. Without an adaptive layer towards the sample,

however, successful measurements were not achieved. A thin silicone layer provided better adaption, yet no results were obtained. It was concluded that the curvature arising through the arc holding device distorts the Laser. When flat on a sample, the stiff silicone layer yielded data. It is in the author's opinion that the arc approach should eventually allow 3D, confocal, refraction free and sample protecting Raman microscopy automatically and under high vacuum conditions. This approach, however, would have to be adapted significantly calling for further research.

9 Appendix

9.1 Setup

The Raman microscope used in this thesis is a LABRAM HR 800 Raman microscope which can be seen in Figure 9.1. It uses a red Laser (wavelength: 632,81 nm, power: 16 W) by default, but can introduce external Lasers. Mostly used in this thesis was the green Laser (wavelength: 532,16 nm, power: 50 W from the company *Laser Quantum*[7]. The resolution of the microscope depends on the used grating. By default, the LABRAM HR has two gratings; their resulting resolution (depending on the used laser) can be seen in Table 9.1. With this setup a Raman spectrum of a sample, in the place the Laser beam is focused can be taken.

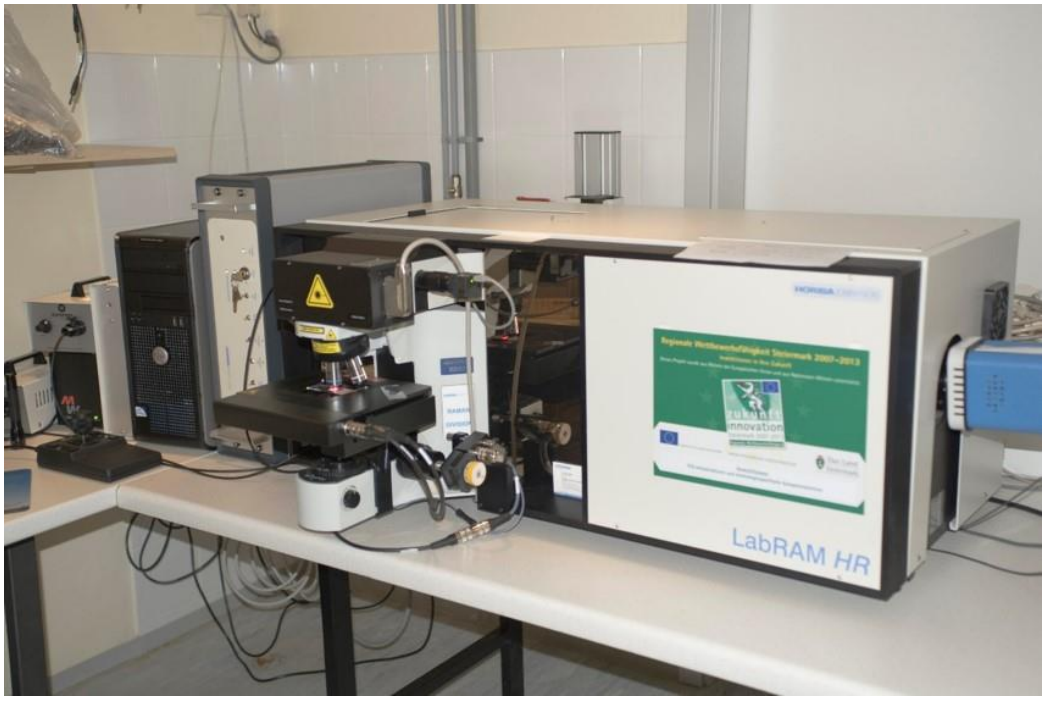

Figure 9.1: A LABRAM HR 800 Raman microscope which was used for this thesis, located at FELMI/ZFE Technical University Graz, Austria.

[7] www.laserquantum.com

Table 9.1: Resulting resolution of the LABRAM HR 800 Raman microscope depending on used La-ser and used grating.

	Grating	
Laser	300 l / mm	1800 l / mm
red (632,81 nm)	5 cm^{-1}/px	0,9 cm^{-1}/px
green (532,16 nm)	3 cm^{-1}/px	0,37 cm^{-1}/px

9.2 Measurement parameters

Every spectrum presented in this thesis was obtained with the following settings unless otherwise noted.

General settings:	Laser:	green	(532,16 nm)
	grating:		300 l/mm
	slit:		100
	hole:		200
	accumulations:		2
	oil objective:		100x

For each individual measurement and sample, the Laser intensity and integration times were adjusted accordingly to be suited to the material and receive similar intensity count.

Settings that differ from spectrum to spectrum are listed below each figure.

9.3 List of figures

9.4 List of tables

9.5 References

[1] C. V. Raman, *The molecular scattering of light*. University of Calcutta, 1922.
[2] R. Salzer and H. W. Siesler, *Infrared and Raman Spectroscopic Imaging*. John Wiley & Sons, 2014.
[3] D. J. Gardiner and P. R. Graves, Eds., *Practical Raman Spectroscopy*. Berlin Heidelberg: Springer-Verlag, 1989.
[4] T. Dieing, O. Hollricher, and J. Toporski, *Confocal Raman Microscopy*. Berlin, Heidelberg: Springer, 2011.
[5] N. J. Everall, 'Confocal Raman microscopy: common errors and artefacts', *The Analyst*, vol. 135, no. 10, p. 2512, 2010, doi: 10.1039/c0an00371a.
[6] N. Sultanova, S. Kasarova, and I. Nikolov, 'Dispersion Properties of Optical Polymers', *Acta Phys. Pol. A*, vol. 116, no. 4, pp. 585–587, Oct. 2009, doi: 10.12693/APhysPolA.116.585.
[7] N. Everall, 'Optimising image quality in 2D and 3D confocal Raman mapping: 2D and 3D Raman imaging', *J. Raman Spectrosc.*, vol. 45, no. 1, pp. 133–138, Jan. 2014, doi: 10.1002/jrs.4430.
[8] H. Tang *et al.*, 'Estimation of Refractive Index for Biological Tissue Using Micro-Optical Coherence Tomography', *IEEE Trans. Biomed. Eng.*, vol. 66, no. 6, pp. 1803–1809, 2019, doi: 10.1109/TBME.2018.2885844.
[9] J. P. Tomba and J. M. Pastor, 'Confocal Raman Microspectroscopy: A Non-Invasive Approach for in-Depth Analyses of Polymer Substrates', *Macromol. Chem. Phys.*, vol. 210, no. 7, pp. 549–554, Apr. 2009, doi: 10.1002/macp.200800582.
[10] O. Hollricher, U. Schmidt, and S. Breuninger, 'RISE Microscopy: Correlative Raman-SEM Imaging', *Microsc. Today*, vol. 22, no. 6, pp. 36–39, Nov. 2014, doi: 10.1017/S1551929514001175.
[11] J. Toporski, T. Dieing, and O. Hollricher, *Confocal Raman Microscopy*. Springer, 2018.
[12] Gr. Landsberg and L. Mandelstam, 'Über die Lichtzerstreuung in Kristallen', *Z. Für Phys.*, vol. 50, no. 11, pp. 769–780, Nov. 1928, doi: 10.1007/BF01339412.
[13] C. N. Banwell and E. M. McCash, *Fundamentals of molecular spectroscopy*, 4. ed. London [u.a.]: McGraw-Hill, 1994.
[14] 'Intensities in Raman spectra I. A bond polarizability theory', *Proc. R. Soc. Lond. Ser. Math. Phys. Sci.*, vol. 217, no. 1129, pp. 203–221, Apr. 1953, doi: 10.1098/rspa.1953.0057.
[15] K. J. Laidler and J. H. Meiser, *Physical chemistry*. Benjamin/Cummings Pub. Co., 1982.
[16] D. C. Harris and M. D. Bertolucci, *Symmetry and Spectroscopy: An Introduction to Vibrational and Electronic Spectroscopy*. Courier Corporation, 1989.

[17] T. Schmid and P. Dariz, ‘Raman Microspectroscopic Imaging of Binder Remnants in Historical Mortars Reveals Processing Conditions’, *Heritage*, vol. 2, no. 2, pp. 1662–1683, Jun. 2019, doi: 10.3390/heritage2020102.
[18] A. Farhadian, M. Kavosh Tehrani, M. Keshavarz, and S. Darbani, ‘Raman spectroscopy combined with principle component analysis to investigate the aging of high energy materials’, *Laser Phys.*, vol. 27, p. 075701, Jul. 2017, doi: 10.1088/1555-6611/aa7485.
[19] H. Mitsutake, R. J. Poppi, M. C. Breitkreitz, H. Mitsutake, R. J. Poppi, and M. C. Breitkreitz, ‘Raman Imaging Spectroscopy: History, Fundamentals and Current Scenario of the Technique’, *J. Braz. Chem. Soc.*, vol. 30, no. 11, pp. 2243–2258, Nov. 2019, doi: 10.21577/0103-5053.20190116.
[20] N. Everall, ‘Depth Profiling With Confocal Raman Microscopy, Part I’, p. 6.
[21] N. Everall, ‘Depth Profiling with Confocal Raman Microscopy, Part II’, p. 10.
[22] M. Born and E. Wolf, *Principles of optics: electromagnetic theory of propagation, interference and diffraction of light*, 7th expanded ed. Cambridge ; New York: Cambridge University Press, 1999.
[23] K. Uchinokura, T. Sekine, and E. Matsuura, ‘Raman scattering by silicon’, *Solid State Commun.*, vol. 11, no. 1, pp. 47–49, Jul. 1972, doi: 10.1016/0038-1098(72)91127-1.